INJECTION LOCKED SEMICONDUCTOR LASER DIODES

FOR HIGH SPEED OPTICAL COMMUNICATION

BY

MOHAMED ADEL SHEMIS

A Thesis Presented to the

DEANSHIP OF GRADUATE STUDIES

KING FAHD UNIVERSITY OF PETROLEUM & MINERALS

DHAHRAN, SAUDI ARABIA

In Partial Fulfillment of the
Requirements for the Degree of

MASTER OF SCIENCE

In

ELECTRICAL ENGINEERING

May 2017

KING FAHD UNIVERSITY OF PETROLEUM & MINERALS

DHAHRAN- 31261, SAUDI ARABIA

DEANSHIP OF GRADUATE STUDIES

This thesis, written by **MOHAMED ADEL SHEMIS** under the direction of his thesis

advisor and approved by his thesis committee, has been presented and accepted by the

Dean of Graduate Studies, in partial fulfillment of the requirements for the degree of
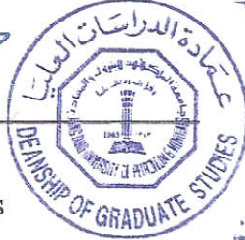
MASTER OF SCIENCE IN ELECTRICAL ENGINEERING.

Dr. Ali Al-Shaikhi
Department Chairman

Dr. Salam A. Zummo
Dean of Graduate Studies

Date _28/5/17_

Dr. Mohammed Zahed M. Khan
(Advisor)

Dr. Khurram K. Qureshi
(Member)

Dr. Samir Al-ghadban
(Member)

Dedicated to

my beloved parents, Dr. Adel Shemis and Mrs. Omaima Keshk

my sisters, Dr. Sara Shemis and Ms. Dina Shemis

my brothers, Dr. Mahmoud Shemis and Ahmed Shemis

ACKNOWLEDGMENTS

TABLE OF CONTENTS

LIST OF TABLES

LIST OF FIGURES

LIST OF ABBREVIATIONS

AMP	:	Amplifier
ASE	:	Amplified Spontaneous Emission
AWG	:	Array Waveguide Grating or Arbitrary Wave Generator
BER	:	Bit Error Rate
BLS	:	Broadband Laser Source
BPF	:	Band Pass Filter
BS	:	Beam Splitter
BTB	:	Back-To-Back
CAPEX	:	Capital Expenditure
CP	:	Coupler
CW	:	Continuous Wave
DCA	:	Digital Communication Analyzer
Demux	:	Demultiplexer
DMT	:	Discrete Multi-Tone
DP-16QAM	:	Dual Polarization 16 Quadrature Amplitude Modulation
DP-IQM	:	Dual-Polarization In-Phase-And-Quadrature Modulator
DP-QPSK	:	Dual-Polarization Quadrature Phase Shift Keying
DQPSK	:	Differential Quaternary Phase-Shift Keying
EAM-SOA Amplifiers	:	Reflective Electroabsorption Modulator- Semiconductor
EDFA	:	Erbium Doped Fiber Amplifier
FEC	:	Free Error Correction
FP	:	Fabry-Perot
FPLD	:	Fabry Perot Laser Diode
FSO	:	Free Space Optics
FSO	:	Free Space Optical Communication
GBd	:	Giga Baud

HD	:	High Difinition
IR	:	Infrared
L	:	Length
LD	:	Laser Diode
LED	:	Light Emitting Diode
LO	:	Local Oscillator
MBE	:	Molecular Beam Epitaxy
MUX	:	Multiplexer
MZM	:	Mach-Zehnder Modulator
NG-PONs	:	Next Generation-Passive Optical Networks
OAM-QPSK	:	Orbital Angular Momentum Quadrature Phase Shift Keying
OC	:	Optical Circulator
OFDM	:	Orthogonal Frequency-Division Multiplexing
OLT	:	Optical Line Terminal
OMA	:	Optical Modulation Analyzer
ONU	:	Optical Network Unit
OOK	:	On-Off-Keying
OSA	:	Optical Spectrum Analyzer
OSA	:	Optical Spectrum Analyser
OTF	:	Optical Tunable Filter
PC	:	Polartization Controler
PD	:	Photo-Detector
PDM	:	Polarization-Division Multiplexing
PON	:	Passive Optical Network
PRBS	:	Pseudo-Random Bit Sequence
QAM	:	Quaadrature Amplitude Modulation
QDash	:	Quantum Dash
QDot	:	Quantum Dot
QWell	:	Quantum Well

RCLEDs	:	Resonant-Cavity Light Emitting Diodes
RF	:	Radio Frequency
RGB	:	Red Green Blue
RN	:	Remote Node
RSOA	:	Reflective Semiconductor Optical Amplifiers
Rx	:	Receiver
SCH	:	Separately Confined Hetero-Structure
SMF	:	Single Mode Fiber
SMSR	:	Side Mode Suppression Ratio
SNR	:	Signal To Noise Ratio
SPW	:	Short Pulse Width
TBPF	:	Tunable Band Pass Filter
TE	:	Transverse Electric
TEC	:	Theroelectric Cooler
TLS	:	Tunable Laser Source
TM	:	Transverse Magnetic
Tx	:	Transmitter
VLC	:	Visible Light Communication
VOA	:	Variable Optical Attenuator
W	:	Width
WDM	:	Wavelength Division Multiplexing
WFP	:	Weak-Resonant Cavity

ABSTRACT

Full Name   : Mohamed Adel Shemis

Thesis Title   : Injection Locked Semiconductor Laser Diodes for High Speed Optical Communication

Major Field   : Electrical Engineering

Date of Degree : May 2017

Recently, there has been a rising demand on high bandwidth multi-subscriber optical wavelength division multiplexed passive optical networks due to the ever increasing exchange of information. Hence, light sources employed in these networks are crucial and requires to be cheap, high-speed and energy efficient. In this respect, recently demonstrated broadband laser sources based on quantum-dash active region in C - and L –band wavelength window were found to be promising candidates for multi-terabits/s date transmission and next-generation passive optical networks. The inherent broad stimulated emission could be exploited to serve several subscribers using a single source which is the subject of this this work.

First, a tunable subcarrier self-injection locked InAs/InP QDash LD, with ~11 nm tunability and covering ~ 18 subcarriers in the L-band regime at the wavelength range 1600-1610 nm was demonstrated with a comprehensive investigation on the locked mode wavelength tunability, stability, mode power, and side mode suppression ratio. Moreover, the self-locked QDash LD was demonstrated as a multi-wavelength source capable of producing selective number of subcarriers of Fabry-Perot modes from 1 to 16.

Next, using a single self-locked mode of the QDash LD as a single subcarrier, we demonstrated up to 128 Gb/s and 176 Gb/s optical communication through 20 km and 10 km SMF, respectively, using dual-polarization quadrature phase shift keying (DP-QPSK) modulation scheme. Moreover, a minimum of 100 Gb/s transmission is demonstrated within the ~11 nm wavelength tunability of the self-locked QDash laser. We further proposed a multi-subscriber WDM-PON based on a self-injection locked QDash LD as a unified down-streaming multi-wavelength source that would significantly reduce the system cost and simplify the design and implementation. The system has a potential to reach can reach up to ~2 Tb/s transmission capacity. Furthermore, we demonstrated an indoor L-band free space optical (FSO) communication based on a tunable self-injection locked QDash LD with a maximum data rate of 176 Gb/s over 16 m free space optical channel and using DP-QPSK modulation scheme

Lastly, we investigated external injection locking of blue InGaN/GaN commercial LD with focus on SMSR, peak power, injection power and stability. We demonstrated visible light communication based on directed modulated blue LD using OOK scheme, reaching up to 2 Gb/s data rate. This substantiates utilizing of visible light communication (VLC) as a substitution for IR communication with dual feature of indoor communication and illumination.

ملخص الرسالة

الاسم الكامل: محمد عادل جودة شميس

عنوان الرسالة: حقن مغلق لليزرات أشباه الموصلات لإتصالات بصرية عالية السرعة

التخصص: هندسة كهربائية

تاريخ الدرجة العلمية: مايو 2017

يزداد الطلب في الآونة الأخيرة على شبكة الاتصالات الضوئية متعددة المستخدمين لزيادة الطلب على تبادل المعلومات الرقمية. لذا فإن مصادر الضوء لها دور كبير في رفع كفاءة هذه الشبكة ويتطلب أن تكون رخيصة وسريعة الاستجابة وموفرة للطاقة، لذا فقد تم دراسة مصادر ليزر فائقة العرض معتمدة على الخطوط الكمية في نطاق التصال L & C، كمصادر واعدة لاتصال ذو سرعة بيانات تفوق تصل إلى multi-Tb/s. يمكن استغلال البث المحفز العريض لهذه الليزرات لخدمة عدة مستخدمين باستخدام مصدر ضوئي واحد وهو ماتم دراسته في هذه الرسالة.

تم دراسة الحقن المغلق الذاتي لليزر الخطوط الكمية InAs/InP كمصدر حامل للبيانات قابل للضبط مع نطاق يساوي 11 nm، ومكون من 18 حاملة للبيانات في النطاق الضوئي L عند الطول الموجي 1600-1610 nm، مع التكيز على نطاق الضبط والثبات والقدرة الضوئية، وSMSR. كما تم دراسته كمصدر ضوئي متعدد الحوامل مع عدد يتراوح ما بين حاملة واحدة و 16 حاملة.

وبعد ذلك، وباستخدام وضع واحد مغلق ذاتيا من ليزر الخطوط الكمية كحاملة بيانات، تم نقل 128 Gb/s & 176 Gb/s خلال 20 km and 10 km من الألياف ذات الوضع الواحد، على الترتيب، باستخدام نضام تعديل DP-QPSK. وعلاوة على ذلك، تم تحقيق سرعة نقل بيانات 100 Gb/s باستخدام حاملة بيانات معتمدة على حقن مغلق ذاتي لليزر خطوط كمية قابلة للضبط في نطاق 11 nm~. كما تم تقديم شبكة إتصالات متعددة المستخدمين معتمدة على ليزر مغلق ذاتي كمصدر متعدد الحوامل لارسال البيانات وهو ما يمكنه خفض تكلفة نظام الإتصالات وتسهل التصميم. شبكة الإتصال المقدمة قادرة على تحقيق سرعة نقل تصل إلى 2 Tb/s~. كما تم بناء اتصال ضوئي في فضاء طوله 16 m في النطاق الضوئي L، معتمدا على ليزر خطوط كمية قابلة للضبط، وباستخدام نظام التعديل DP-QPSK.

وأخيرا، قمنا بالتحقيق في حقن مغلق خارجي لليزر InGaN/GaN أزرق تجاري، مع التركيز على قدرة الوضع، وقدرة الحقن الخارجية وثبات الحقن المغلق وSMSR. كما درسنا اتصالات الضوء المرئي باستخدام تعديل مباشر لليزر الأزرق

باستخدام نظام تعديل OOK، لتصل سرعة الإتصال إلى Gb/s 2. وهذا يدعم استخدام اتصالات الضوء المرئي كبديل للاتصالات الأشعة تحت الحمراء مع ميزة مزدوجة من الاتصالات في الأماكن المغلقة والإضاءة.

CHAPTER 1

INTRODUCTION

1.1 Background

Currently, the need of high bandwidth optical communication networks is intensifying owing to sharp increase in both, the number of end-users, and their demand for high speed mobile and internet connectivity for applications such as High Definition (HD) video materials and 3-D televisions. According to CISCO Inc., the IP traffic is expected to rise from the 1 ZB (10^{21}) in the end 2016 to 2.3 ZB by 2020, with an increase in busy-hour (busiest hour in the day) internet traffic by a factor of 4.6 [1], mainly caused by applications such as TVs, tablets, smartphones, and machine to machine modules [1]. Also, by 2020, wired IP traffic will account for 34 %, and Wi-Fi and mobile devices will account for majority of the IP traffic, 66 %, compare to 52 % of wired IP traffic wired, by 2015 [1]. However, in the following years, there will be more challenges in meeting higher IP. In this respect, wavelength division multiplexed (WDM) system and in particular passive optical networks (WDM-PONs) has the potential to meet the demands of the future high capacity networks. Hence, it is imperative to propose and investigate different network system, transmitters, and in particular light sources, for the next generation passive optical networks (NG-PONs).

1.2 WDM-PON

WDM based passive optical networks (WDM-PONs) is an architecture providing point-to-point connectivity to multiple remote locations, and has been acknowledged as a potential low-cost scheme for next-generation 10G, 100G passive optical networks

(NG-PONs) which are being developed to provide higher bandwidth with better privacy and scalability [2]. Fig. 1 shows a typical schematic of a WDM-PON serving *n* users at the OLT using a feeder line (channel). However, amplified spontaneous emission (ASE) source based optical networks significantly limit the communication bandwidth due to the incoherency and noise intensity, employed in the transmitters. To accommodate the demand on high data rate transmission, semiconductor Fabry Perot laser diode (FPLD) based wavelength division multiplexing passive optical network (WDM-PON) is attractive for its high bandwidth and colorless operation. Moreover, transmitters in optical line terminal (OLT) and optical network unit (ONU) should be energy efficient, and mass producible and deployable, to qualify as a low-cost and potential candidate for NG-PONs [3]. In this respect, extensive research has been carried out with different sources and architecture to satisfy these requirements.
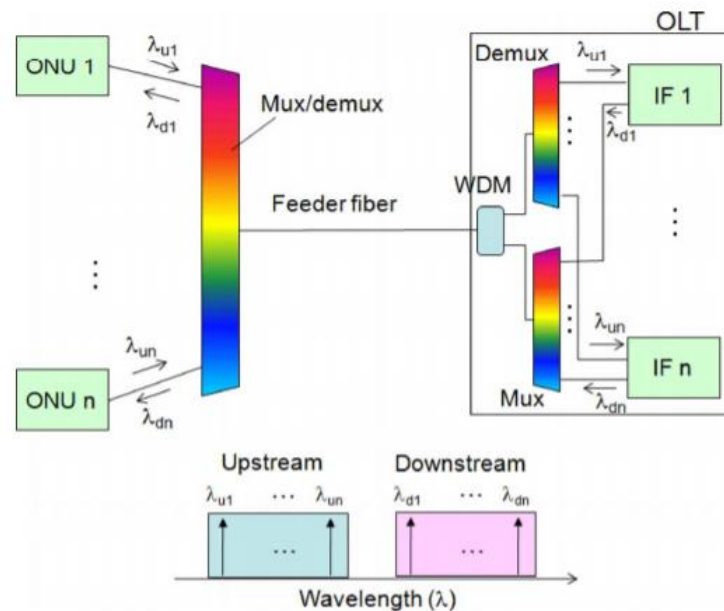
Figure 1: A typical WDM-PON [2]

1.2.1 Semiconductor Laser Sources in WDM-PON

Semiconductor laser diodes features include high emission coherency, small size, relatively low price and long lifetime which make them the optimal choice for several optical applications that require an efficient, coherent, compact optical source. Over the last few decades, laser diodes have proven itself as an efficient source for optical communication systems in both free space and optical fiber channels. The optimal goal of the laser diode is to convert the electron-hole pairs that are pumped by an external electrical source to radiative recombination in order to produce coherent photons. Thus, laser diodes are fabricated using direct bandgap semiconductors since they are much more efficient light emitters than the indirect bandgap semiconductors in order to maximize the radiative recombination. The first invented laser diode in 1962 was a *p-n* diode based. However, the most efficient laser diodes nowadays incorporate the idea of carrier confinement in which electron-hole pairs are confined within double heterostructure configuration to maximize the radiative recombination via carrier confinement. More recently, quantum confined active regions has shown to improve the characteristics of the laser tremendously and has been occupying the center stage in optical communications.

Several WDM-PON architectures employing a variety of light sources have been reported in the literature to address NG-PONs, however, injection-locked WDM-PONs are found to be highly attractive owing to their "colorless" feature enabling dynamic wavelength allocations to the subscribers [3]. Many direct modulated light sources for WDM-PON have been reported such as reflective semiconductor optical amplifiers (RSOA) [4], reflective electroabsorption modulator- semiconductor amplifiers (EAM-SOA) [5], Fabry-Perot laser diodes (FP-LD) [4], weak-resonant cavity FP-LD (WFP-LD) [6], however, their bandwidth is found to be limited to 10 Gb/s, and they become

cost-ineffective as the number of multi-subscribers increase, particularly for FP-LSs and WFP-LDs.

1.2.1.1 Quantum Dash Laser Diodes (QDash LD)

InAs/GaAs quantum dots (QDots) and InGaAsP/InP quantum well (QWells) laser diodes provide a very efficient laser source due to their excellent performance in infrared emission, with broader lasing spectrum [4, 7] in the former case due to inherent inhomogeneity of the QDots size. However, in optical network systems, InAs/GaAs QDot based laser diodes is struggling to cover C, L and U wavelength communication bands. Thus, a lot of research has been devoted on InAs/InP QDots and quantum dashes (QDashes) with the former one requiring assisting growth technique to realize while the latter inherently grows on InP substrate, and hence is the logical choice to address the future optical communication system requirements. QDashes have excellent attributes in C and L-band such as high saturation power and fast response [7, 10, 11]. However, the orientation of the QDashes in the laser cavity with respect to the cavity and facets directions play a vital role in determining the polarization modes within the cavity [6, 8]. In [10], the authors reported that either TM or TE modes can be the dominating mode of the lasing spectrum by changing the orientation of the grown dash elongation being parallel or perpendicular to the laser facet, respectively. They also have shown that by changing the orientation of dashes they could blue shift the lasing center wavelength when dash elongation is perpendicular to the laser facet on the cost of a gain reduction.

QDash in $In_{1-x}Ga_xAl_yAs_{1-y}$ quantum well structures are usually grown for operation at the C and L-bands to enhance better carrier confinement. The emission wavelength and hence the bandgap energy of the device depends on the composition ratios of GaAs,

AlAs, and InAs, as shown in Fig. 2. The lines connecting these binary compounds represent the case when only two compounds are combined, whereas the space between the lines of the figure represents $In_{1-x}Ga_xAl_yAs_{1-y}$ material, however it is preferred to be as close as possible to the solid lines (direct gap structure). The horizontal lines show the case for emission at 1.3 µm and 1.55 µm for corresponding bandgap energy of 0.9537 eV and 0.7999 eV, respectively [9, 10]. Also, the vertical lines show the composition that have matching lattice constant for materials for *p-n* junction materials.
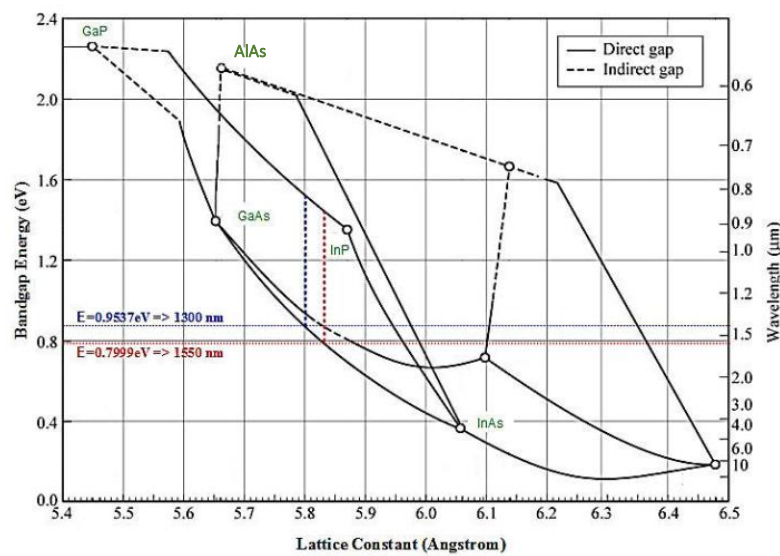
Figure 2: Bandgap characteristics of III-V semiconductors, particularly, $In_{1-x}Ga_xAl_yAs_{1-y}$ at different composition ratios.

Different laser diode structures with multiple layers of InAs QDashes grown on InP substrate have been reported with emission wavelengths in C and L-bands [15, 16] separated by quantum barrier layers of fixed thickness. Moreover, in general, the grown QDashes are random in size and composition leading to substantial broadening of the emission spectrum due to dispersive optical transitions in the active region. This degrades the coherency of the laser emission and also the performance. However, on other front, this broadband emission spectrum could be exploited to realize multi-wavelength lasers [17] and in fact QDash LDs with chirped active region have been

reported in which the barriers have different thicknesses in order to have different degrees of carrier confinement potential (due to inhomogeneous growth of QDashes in each dash layer as a result of varying strain experienced by each dash layer) and thus contributes to broader lasing spectrum [8, 18].

1.2.1.2 QDash LD Based Optical Communication

Recently, FP-LD based on QDash active region, which possess inherently broad lasing emission, has been exploited as an external seeding light source to injection-lock 16 modes of a typical narrow band FP-LD [19] in C – band regime (1552 – 1562 nm) with 40 Gb/s capacity. More recently, deployment of injection-locked far L – band QDash LD as a unified transceiver in NG-PONs was proposed, exploiting the spectrum beyond C – band under the NG-PONs expanded spectrum wavelength plan, with ~20 nm tunability. Moreover, 100 Gb/s externally modulated DP-QPSK transmission was reported from a single ~1621 nm channel over 10 km SMF [20].

In general, broadband QDash LDs suffer from incoherency in the FP mode, rendering the utilization of their FP modes as a subcarrier difficult. Moreover, it was reported that the linewidth of the FP mode is in the range of tens of MHz [31, 32] beside being incoherent. Therefore, going to higher modulation schemes, particularly phase modulations was difficult and hence a competing mode locking scheme was utilized by CNRS France group which exploited the inherent inhomogeneous nature of QDashes and reported single section or self-pulsating mode locked QDash wherein the phase of all the FP modes are locked to substantially improved its characteristics. Besides, self-homodyne detection technique was also proposed and demonstrated as an alternate solution in optical communication [17]. In this method, a copy of the subcarrier used for detection is also transmitted along with the information signal. In [24] different

polarization was utilized to transmit the carrier and the information signal as shown in Fig. 3. Although, this technique will limit the transmission rate due to the utilization of the second polarization for sending the local oscillator, it has the advantage of not requiring a local oscillator at the receiver. The group employed mode locked QDash LD to filter out a single FP mode for communication via 75–km fiber to achieve a transmission rate of 72 Gbit/s.
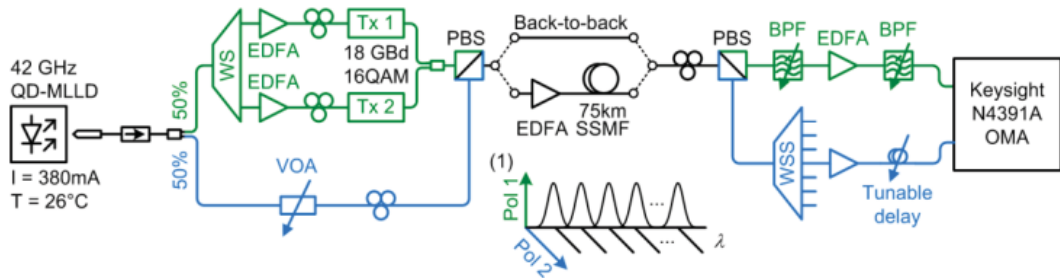
Figure 3: Self-homodyne WDM system using a single mode locked QDash LD as a source for multiple subcarriers [17].

1.2.2 Multi-Wavelength Sources

Coherent and stable multi-wavelength source or frequency combs have also been identified as a potential source in the next generation wavelength-division-multiplexed passive optical networks (WDM-PONs), since sources usually determine the communication bandwidth and performance of the system. Therefore, several frequency combs sources have been widely reported as solution to adopt in cost-effective WDM-PON such as fiber lasers, phase- and intensity-modulated sources [23]. However, these methods utilize incompact designs and would require expensive components. On other hand, mode locked QDash LDs, discussed in the previous section, has been proposed and tested as an effective multi-wavelength source with 23 and 60 subcarriers for 190 Gb/s and 100 Gb/s communication per channel. This WDM system was reported with C-band laser and using external modulation scheme [24, 25].

Fig. 4 shows the experimental setup for WDM system based mode-locked QDash LD with a single source providing a frequency comb with 12 Tbit/s (32QAM 60×20 GBd PDM) transmission capacity with 60 subcarriers.
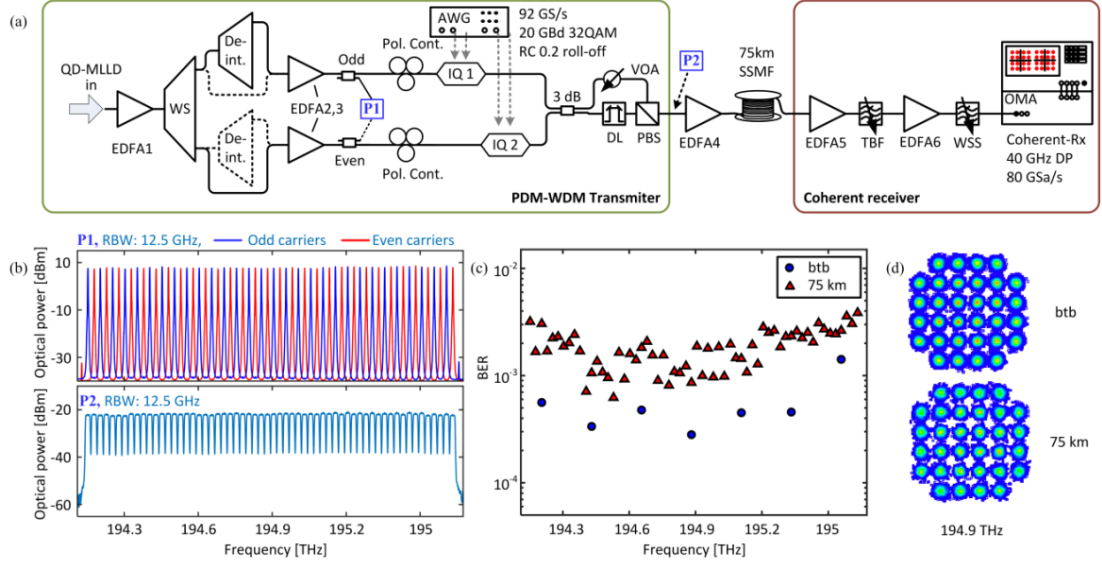
Figure 4: (a) Experimental setup of WDM system based on mode locked QDash LD with resonant feedback. (b) Spectra of the subcarriers before modulation (top), and spectrum of 60 modulated subcarriers (bottom). (c) BER for different carries for BTB and 75 km fiber channels. (d) Constellation diagrams of the comb line at 194.9 THz for BTB and 75 km fiber transmission. Taken from [25].

1.3   Injection Locked WDM-PON

One of the challenges to achieve high bandwidth in FPLD based optical communication systems and WDM-PONs is to tune the FPLD to lase at one single FP mode, similar to distributive feedback or distribute Bragg reflector lasers. The former ones are cost-effective and hence are preferred choice compared to latter ones. Hence, injection locking technique was proposed and demonstrated as a coherency-boosting technique, which not only improved the modulation capability of the FL-LDs but also assisted in realizing colorless WDM-PONs that are more user-friendly with dynamic allocation of the upstreaming and downstreaming subcarrier wavelength for operation. There are two approaches for injection locking technique, one is using an external seeding source

8

which is used to lock the frequency and phase of a particular single FP mode of the slave FP LD, thereby amplifying the mode while suppressing the other side modes. The other scheme is self-injection locking in which one single FP mode of a laser is filtered out and fed back into the laser, to force locking of the frequency and phase of that particular mode besides amplifying it and suppress the other side modes. However, external injection locking would require a costly external master laser which would translate into bulky, energy hungry, and expensive system architecture. On the other hand, self-injection locking is a cost-effective compact technique and more flexible in terms of FP mode tunability. Both of these techniques have been reported in literature addressing colourless WDM-PONs using various class of FP LDs to increase the communication bandwidth of several FP modes and hence the bandwidth reaching end users.

1.3.1   External Injection Locking

External injection-locking have been reported in literature using external seeding source in the form of BLS [26] or tunable laser source (TLS) [27], to select a particular FP mode as a subcarrier while suppressing the other modes of a multimode FP LD transmitter. Injection locking using a TLS (BLS) enabled a successful upstream transmission of 10 Gb/s (2.5 Gb/s) 16 QAM-OFDM (ON-OFF keying) signal over 60 (20) km SMF by employing weak resonant-cavity FP-LDs (WRC-FP-LD) [4]. A data capacity of 80 Gb/s is demonstrated by this FP-LD with a tunability of 32 channels (~1530 – ~1560 nm) in the C-band. Moreover, employment of FP-LDs as master-slave-pair was proposed in [28] for cost-effective injection-locked WDM-PONs with a tunability of 34 nm in C – band. Consequently, a 560 Gb/s (20 Gb/s × 28 channels) data capacity was demonstrated using this configuration by QAM-OFDM transmission over 25 km SMF in near L-band (1575 – 1588 nm) [6]. Moreover, reflective semiconductor

optical amplifier (RSOA) at the ONU, with uplink transmission up to 25 Gb/s over 120 km SMF, have also found to be appealing candidates for wavelength reuse PONs with large network capacity [4]

Fig. 5 shows the injection locking in FPLD based optical communication systems [29]. As can be seen in the figure that injection locking led to the suppression of all of the side modes with SMSR of about 30 dB by controlling a tunable laser source to injection-lock only a specific FP mode, which enabled a transmission rate of 10 Gbit/s using 16 QAM modulation. The provided design utilized a master source (tunable laser source) at the transmitter side. However, this design requires several tunable laser sources at the transmitter terminal, one TLS for each channel, which renders its usage impractical. Alternatively, Fig. 6 shows another WDM-PON architecture in which an OLT with n number of FPLDs and channels are injection locked by utilizing only one single broadband light source (BLS). The single broadband light source is sliced using an array waveguide grating (AWG) filter, that also works as a multiplexer (MUX), to injection lock the corresponding FP mode of each channel [2, 21]. This design enables a transmission rate of 20 Gb/s with BER below the FEC limit through utilization of orthogonal frequency division multiplexing OFDM - 16 QAM modulation scheme. In [31], the authors introduced a new design of wavelength reuse in which the downstream modulated light was used to injection lock a FP-LD in the ONU for upstream signal. This substantially improved the system capacity, however, requires RSOAs to be operated in saturation region, as the source for up-streaming.
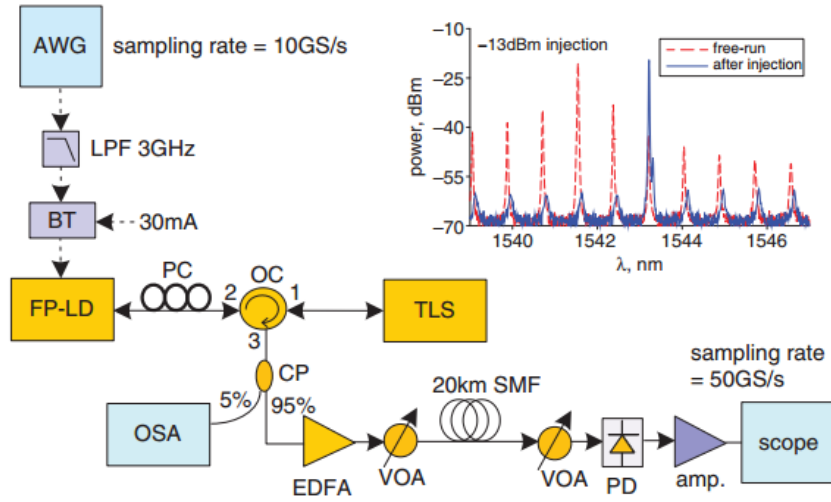
Figure 5: External injection locked FP-LD in optical communication system, at the transmitter terminal [29].
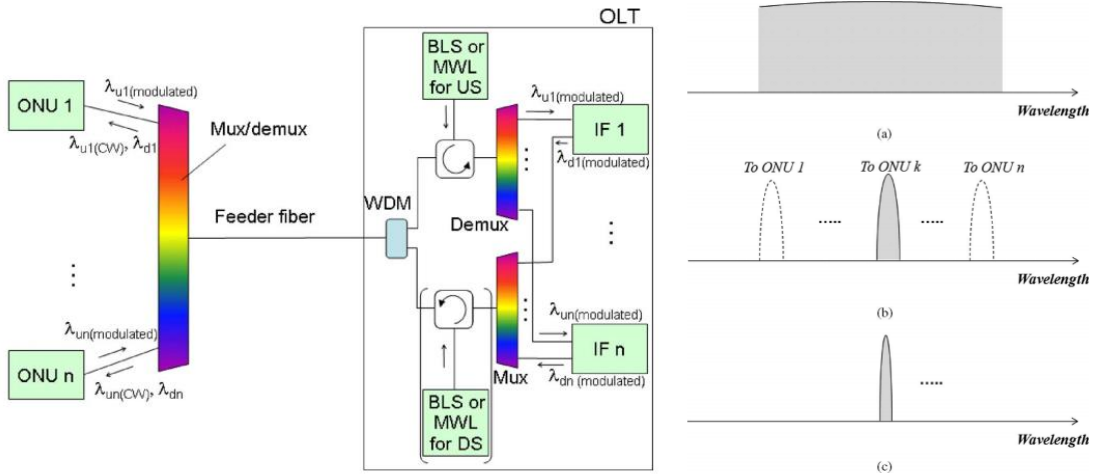
Figure 6: Left: schematic diagram of an optical network system that is based on external injection-locked FP LD using seeding BLS and MUX. Right: optical spectrum of the BLS (top), the sliced spectrum after MUX and demultiplexer (DEMUX) (middle) and the injection locked FP mode (bottom) [3].

1.3.2 Self-Injection Locking

Self-seeded (self-injection locked) colorless PONs, which does not require external seeding sources, has also been actively investigated using RSOA [32] and FP-LDs [33, 34] as a promising low-cost solution for NG-PONs. Different schemes have been proposed in literature to achieve self-seeded PONs. For instance, by employing a tunable band pass filter (TBPF) and an amplifier in the remote node (RN), a 1.25 Gb/s

11

upstream transmission of OOK signal over 21 km SMF was demonstrated by self-seeded RSOA with ~6 nm tunability (1554–1560 nm) [32]. On the other hand, references [24, 25] exploited TBPF in the ONU and Faraday's rotating mirror in RN, respectively, for demonstration of 2.5 Gb/s uplink transmission by self-locked FP-LD with ~20 nm tunability (1536–1556 nm). Ref. [34, 35] demonstrated a self-injection locked FPLD based WDM-PON shown in Fig. 7, The self-locking was implemented using a coupler, a fiber mirror, MUX working as a BPF in feedback loop. Coherent single FP locked modes were achieved at the OLT from n self-injection FP-LD, and, then, transmitted simultaneously. The proposed system could achieve a transmission rate of 2.5 Gb/s with on-off keying modulation, achieving BER of 10^{-9}. Moreover, sophisticated architecture based on modulation averaging reflector [36] and fiber Bragg gratings [37] has also been utilized in RN for FP-LD self-locking purpose, respectively, with reported data rate of 1.25–10 Gb/s OOK transmission over 20–60 SMF by FP-LD in C – and near L-bands.
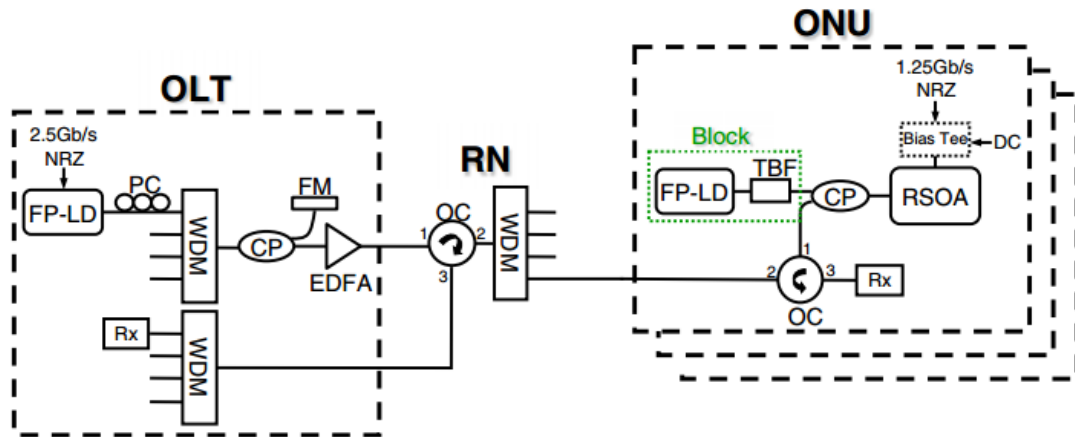
Figure 7: WDM-PON architecture using self-injection locked FP-LDs [35].

1.4 Optical Wireless Communication

Electrical interconnects are currently facing challenges to meet up with the high-speed demands in data centres and high-performance computing, besides electromagnetic

interference problems. In this regard, fiber based optical technologies stand out to be a strong contender presently offering high bandwidth operations. However, this scheme provides a static interconnection within and across the racks, and card-to-card with thousands of kilometres of fiber running in the centres. Hence free-space optical wireless communication (FSO) has been identified as a complementing solution offering better flexibility via providing dynamic interconnects, for efficient operations. Moreover, FSO is also garnering attention in the outdoors as a substitute for optical fiber communications. The interest in this optical technology is further strengthened by its low initial capital expenditure (CAPEX), wide-licence free wavelength domain, and high-level security. Moreover, FSO has the capacity to address various applications, for instance, first/last mile access, terrestrial applications, network access to remote area, under sea and space communications, etc.

1.4.1 Free Space Optical Communication

On the research aspect, data rates up to 400 Gb/s and 320 Gb/s via outdoor 120 m and 11.5 m FSO channel have been reported at 1550 nm utilizing 4 orbital angular momentum quadrature phase shift keying (OAM-QPSK) beams [37] and dual polarization 16 quadrature amplitude modulation (DP-16QAM) scheme [38], respectively. On the other hand, short indoor FSO links of 1 − 6 m, is reported in [39] with 10 − 100 Gb/s data rates and QPSK modulation scheme using C-band laser diodes. Ref [40] targeted card-to-card optical communication and demonstrated 40 Gb/s transmission over 30 cm channel distance at 1550 nm. Very recently, we demonstrated 100 Gb/s over 4 m indoor FSO link at 1621 nm employing a new class of QDash LD with external injection locking scheme [41]. The long wavelength operation of this laser offers possibility of less scattering loss in free space compared to C-band counter parts. Besides, the broadband lasing spectrum feature could be exploited as a tunable laser

source via injection locking technique for WDM-PONs, a highly attractive architecture for future last mile access.

1.4.2 Visible Light Communication

Recently, visible light communication (VLC), another form of indoor optical wireless communication, attracted a major research focus as a substitution for IR communication to meet the demand on high speed and high bandwidth communication [38], and relieve the load on RF and IR wireless networks [39]. Advantages of VLC include network security (blocking the visible light by obstacles means no access to your data), unlicensed spectrum, low power consumption, nonexistence of electromagnetics with other systems and RF systems. Thus, VLC found many applications inside buildings [40], airplanes [41], traffic [42], satellite [43] and underwater conditions [38][44].

LEDs has attracted research attention to be utilized in both VLC and lightening due to many advantages such as their low power consumption, low cost, high efficiency, and long lifetime [40]. However, LEDs have several disadvantages that limits their bandwidth modulation around hundreds of MHz, such as incoherency, slow time response due to their long spontaneous radiative lifetime [45], nonlinearity [46], large parasitic capacitance. Some solutions have been reported in the literature to boost their bandwidth such as equalization at the transmitter (Tx) and receiver (Rx) sides to cancel the parasitic capacitance effect, using spectrally efficient modulation techniques, e.g. Orthogonal Frequency Division Multiplexing (OFDM) [38] and Discrete Multi-Tone (DMT), that could give improvements up to 3 Gb/s for LED based on phosphor-coated single emission and 3 Gb/s for RGB LED [47]. Also, other solutions include the usage of faster LEDs such as resonant-cavity light emitting diodes (RCLEDs), or µLED [48]

that exhibits higher modulation bandwidths due to higher current densities, or RGB LEDs to tribble the data rate.

LDs are also gaining attention as alternate source for VLC due to their coherency, high power, that make them capable of reaching up to 2 Gb/s bandwidth and much higher modulation bandwidth [49]. Using the two modulation schemes, on-off-keying (OOK) [50], and 64-QAM OFDM [51], VLC communication achieved 2.5 Gb/s and 9 Gb/s data rates, respectively. Using a white light based on a phosphor and a blue-LD, 16QAM OFDM modulation scheme was achieved at 4 Gb/s data rate [38].

1.5 Research Contribution

The contribution of this research work is summarized in the following points:

- Self-injection locking assisting technique was successfully utilized, for the first time, to the best of author's knowledge, to demonstrate a widely tunable InAs/InP QDash LD in the mid L-band and covering 1600 nm-1610 nm regime.

- A QDash LD self-injection locked multi-wavelength laser is reported with selective number of subcarriers between 1 and 16.

- A data rate of 44 Gbaud (176 Gb/s) utilizing DP-QPSK modulation scheme, employing a single self-locked FP mode of QDash LD in the L-band, is reported over 10 km SMF transmission and 16 m indoor free space optical (FSO) channel.

- External injection locking on commercial blue InGaN/GaN LD is comprehensively investigated and reported for data rate of up to 2 Gb/s transmission over BTB configuration using OOK scheme.

1.6   Thesis Organization

Chapter 1   is an introductory chapter discussion about the background of the thesis work with a comprehensive literature review.

Chapter 2   discuss about the device level characterization of two different active regions based QDash LD, their comparison, and selection of the optimum device for communication experiments.

Chapter 3   comprehensively covers the detailed characterization of self-injection locked QDash LD as a tunable single wavelength source and a selective multi-wavelength source. In particular, tunability, stability, SMSR, and hysteresis, is extracted to understand the underlying device capability.

Chapter 4   reports the optical transmission results based on self-injection locked QDash LD through SMF and FSO channels. It shows the utilized experimental set up and transmission performance at different channel lengths and received powers. Also, a proposed WDM-PON based on multi-wavelength self-injection locked QDash LD is discussed.

Chapter 5   highlights the work on VLC and provides the external injection locking characterization of blue LD in terms of tunability, stability, and SMSR, and the BTB transmission results using OOK modulation scheme.

Chapter 6   summarizes the thesis work, and provide possible future extension that could potentially be carried by next pool of students.

CHAPTER 2

DEVICE LEVEL CHARACTERIZATION

2.1 Introduction

Performance of a fixed barrier height InAs/InP quantum dash (QDash) with different dash elongation direction along the FPLD cavity was evaluated in terms of lasing center wavelength, internal quantum efficiency and internal loss. These different device structure based QDash laser diodes, namely fixed barrier thickness and chirped barrier thickness, were studied in both pulsed and continuous wave current operations to find the optimum devices that could be utilized as sources in optical communication experiments.

2.2 Device Structure of QDash Laser Diodes

Three QDash LDs structures were used in our work. The first structure is chirped barrier thickness QDash in a quantum well laser diodes. The active region consists of four stacks of InAs dashes embedded in 7.6 nm-thick $In_{0.64}Ga_{0.16}Al_{0.2}As$ asymmetric quantum well layers are separated by five barrier layers of $In_{0.50}Ga_{0.32}Al_{0.18}As$ of thicknesses 25 nm, 20 nm, 15 nm, 10 nm and 10 nm form bottom to top as shown in Fig. 8. As discussed earlier, the variation in barrier thicknesses is introduced to broaden the lasing spectrum. The quantum wells structure is further confined by two 200 nm-thick layers of InGaAlAs, which are the separately confined hetero-structure (SCH) for carrier confinement. Following the quantum wells and SCH layers are the p-type and n-type InAlAs materials. The second and third structure consist of four stacks of InAs QDashes embedded in a 7.6 nm-thick $In_{0.64}Ga_{0.16}Al_{0.2}As$ asymmetric quantum well

layers separated by five barrier layers of $In_{0.50}Ga_{0.32}Al_{0.18}As$ with fixed thickness of 10 nm, as shown in Fig. 8. Similarly, the four layers with barriers were again confined within 160 nm and 200 nm thick SCH layers and the whole structure is sandwiched between p-type and n-type InAlAs materials. However, the difference between the second and the third is the direction of the quantum dash elongation. The elongation of dashes is aligned in a direction parallel and perpendicular to the cleaved laser facet in the second and third structures, respectively, as shown in Fig. 9. It is to be noted that the chirped QDash LD followed identical dash orientation as that of the second device. The laser diodes were fabricated utilizing these three laser device structures and cleaved with different laser cavity lengths (L), and three different ridge-width (W = 2 µm, 3µm, and 4 µm), as shown in Fig. 10.
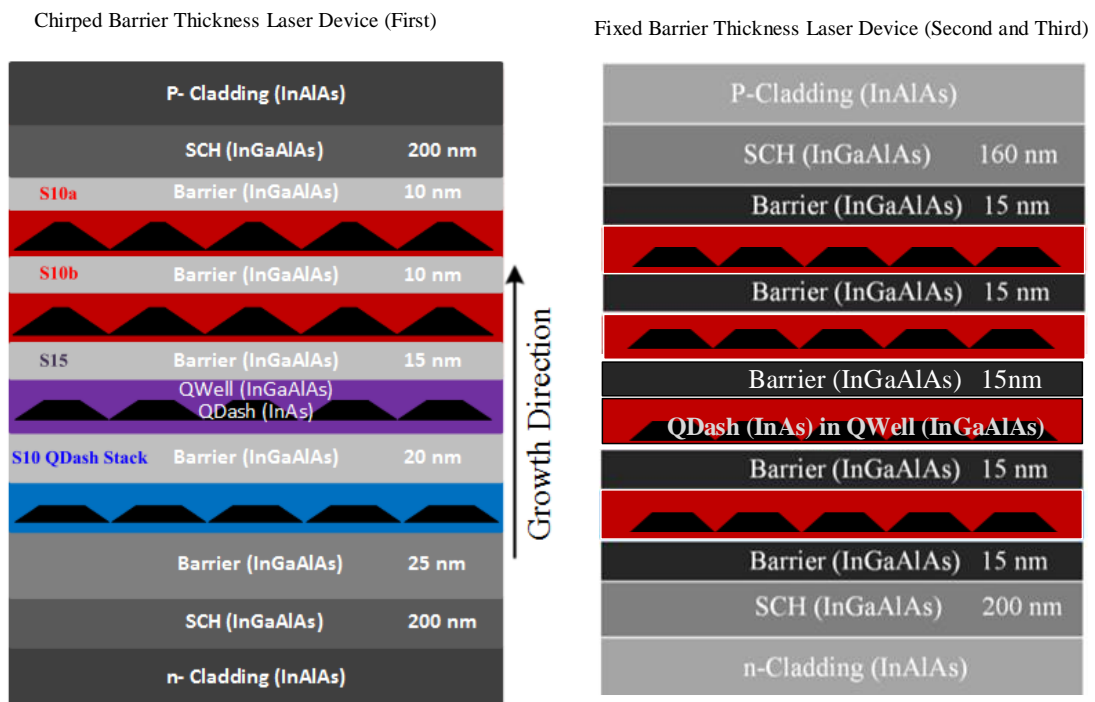
Figure 8: InAs/InP QDash LD structures: Chirped barrier thickness (left: first structure) and fixed barrier thickness (right: second and third structure) studied in this work.
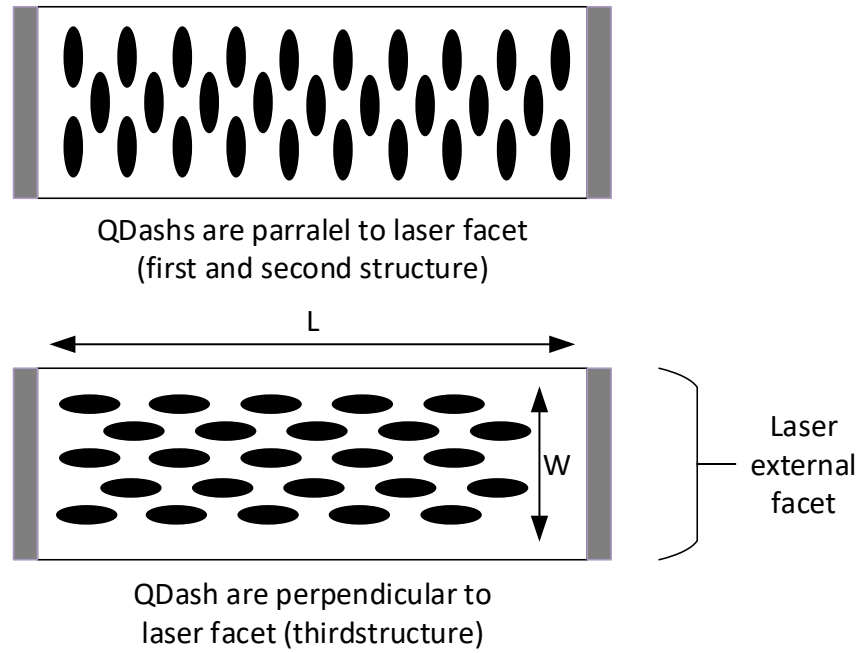
Figure 9: Dash elongation orientation in fixed barrier thickness laser devices being parallel (top: second structure) and perpendicular (bottom: third structure) to the laser facet.
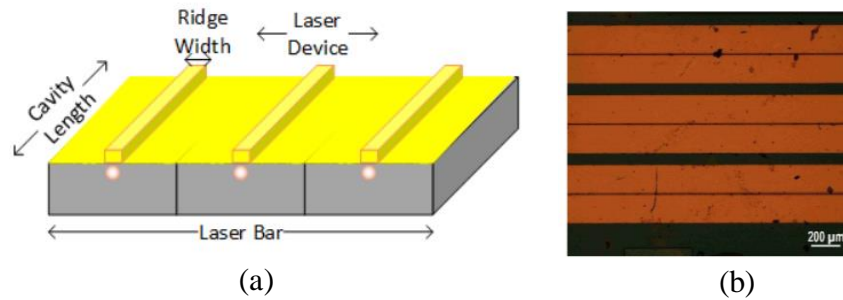
Figure 10: (a) Illustration of a QDash LD bar with several devices, and the labeling of different dimensions, and (b) microscopic image of the fabricated three different ridge-width laser diodes.

2.3 QDash LD Characterization

2.3.1 Fixed Barrier Thickness Laser Diode Characterization

We have characterized fixed barrier thickness QDash LDs with dash elongation being perpendicular to the laser facet (third structure) to be compared with the case where dash elongation is parallel to the facet (second structure) that was fully characterized in our previous group work. The characterization was done with 0.2 % duty cycle pulsed current mode operation. The extracted optical power was measured through a

photodetector at different pulsed injection current and for different laser cavities with fixed ridge width of 4 μm, as shown in Fig. 11. The threshold current and optical slope efficiency ($\Delta P/\Delta l$) were extracted from the optical power versus injection current (*L-I*) curve through linear fitting in the current range of I_{th}-1.5I_{th}. The threshold current density is simply calculated by dividing the threshold current by the active region area L × W.

External quantum efficiency (η_d) is the percentage of extracted optical power to the injected electrons. Whereas, the internal efficiency (η_i) is the ratio of the radiative recombination rate to the generation rate of the electron-hole pairs in the cavity. The differential external quantum efficiency was calculated using

$$\eta_d = \frac{\Delta P}{\Delta l} \cdot \frac{q\lambda}{hc}, \tag{1}$$

where q is the carrier charge (1.602 × 10^{-19} C), λ is the centre wavelength (1680 nm), h is Plank's constant (6.626 × 10^{-34} J·s) and c is the speed of light (m/s), as given in Table 1. The internal quantum efficiency (η_i) in the laser cavity has the expression

$$\frac{1}{\eta_d} = \frac{1}{\eta_i}(1 + \frac{\alpha_i}{\ln(1/R)}L), \tag{2}$$

where α_i (m^{-1}) is the internal loss which is the loss in the generated photons in the laser cavity due to reabsorption and R is the reflectivity of the laser facets (31% in our as-cleaved case). Through linear fitting of the $1/\eta_d$ versus L that is shown in Fig. 12 for the 4 μm ridge width, we could extract both η_i and α_i from the y-intercept and the slope of the line. Table 2 gives the calculated value of η_i and α_i. The measured parameters of third structure QDash LDs were compared with the first structure and second structure of QDash LDs at a cavity length of 800 μm that were characterized earlier by our group, and summarized in Table 2, showing higher threshold current density and

20

internal losses for third structure i.e. dash elongation being perpendicular to the laser facet, attributed to the reduction in the modal gain from the active region. Also, the chirped device (first structure) had blue shifted lasing spectrum near 1610 nm compare to the fixed barrier devices, second and third structures, at 1690 and 1680 nm, respectively. However, when the fixed barrier devices were tested in CW operation, they did not lase and, thus, they were not utilized in optical communication.
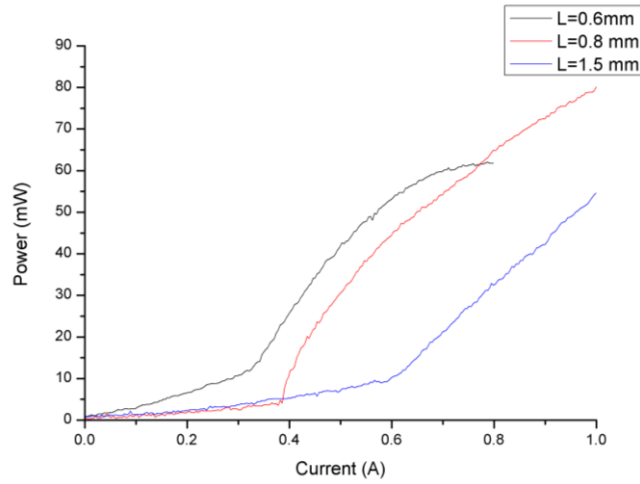
Figure 11: Room temperature L-I characteristics of third device structure at different cavity lengths, and for 4μm ridge-width.

Table 1: Extracted parameters of the third QDash LD structure

Cavity length, L (mm)	Threshold current, I_{th} (A)	Threshold current, I_{th} (A/cm^2)	Optical Efficiency (W/A)	External Quantum Efficiency, η_d (%)	Inverse of External Quantum Efficiency, $1/\eta_d$
0.6	0.326	13583	0.176	48	2.1
0.8	0.386	12063	0.177	48	2.1
1.5	0.603	10050	0.112	30	3.3

21
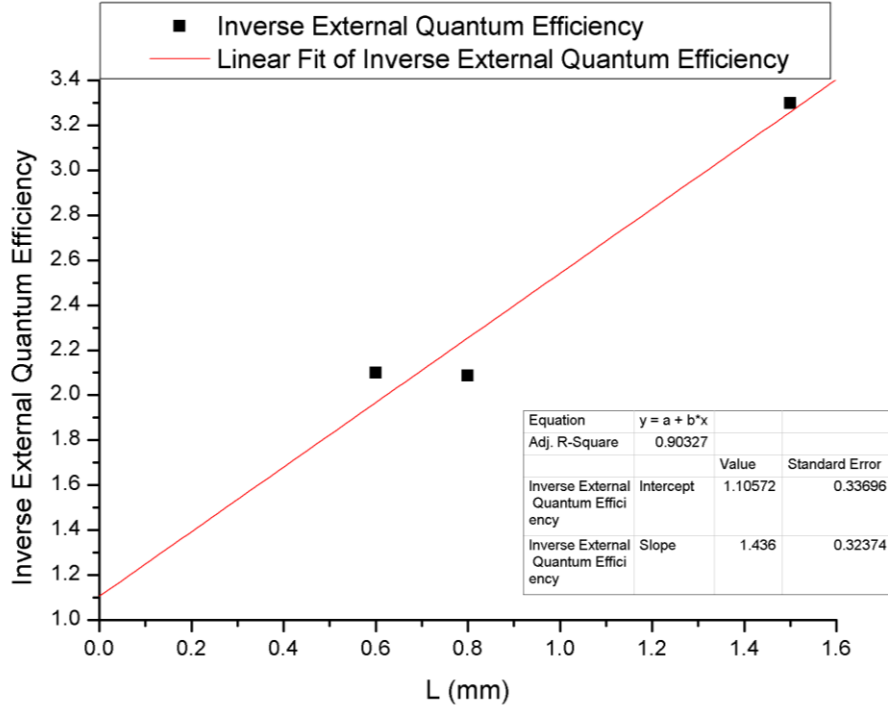
Figure 12: Linearly fitting of $1/\eta_i$ against different cavity lengths for ridge width of 4 μm to extract the internal quantum efficiency and internal loss.

Table 2: Comparison between chirped barrier thickness (first device structure) and fixed barrier thickness (second and third device structure) QDash LDs.

Performance Parameter	Chirped Barriers (First Structure)	Fixed Barriers (Second structure)	Fixed Barriers (Third structure)
$I_{th}(A)$	0.108	0.279	0.386
$J_{th}(A/cm^{-2})$	3146	8743	12063
$\lambda_{emission}$ (nm)	1610	1690	1680
η_i (%)	84	78	90
$\alpha_i(cm^{-1})$	8.9	11	15

2.3.2 Chirped Barrier Thickness Laser Devices Characterization

First device structure QDash LD with a cavity length of 600 μm was tested with 0.2 % duty cycle pulsed current mode operation. The voltage and single facet optical power were measured at 14 °C, as given in Fig. 13. The lasing threshold current was estimated to be 50 mA. Afterwards, the chirped barrier device was tested in CW mode and found

22

to lase in this current operation, as given in the *L-I-V* characteristics in Fig. 14. Thus, it was utilized in the self-injection locking and optical communication experiments. The lasing power was butt coupled into a lensed single mode fiber with 5 % coupling ratio (-13 dB) which is our experimental best coupling at one single facet. The free running lasing spectrum was observed via 0.06 nm resolution optical spectrum analyser (OSA), as shown in Fig. 15. The single facet fiber coupled power was ~0.40 mW at an operating current of $1.1I_{th} = 110$ mA, and at 14 °C controlled heatsink temperature. A fixed cavity length, operating current and temperature were selected due to the limitation of the L-band erbium doped fiber amplifier utilized in the transmission experiments in order to have the majority of the lasing spectrum within 1610-1620 nm wavelength band.
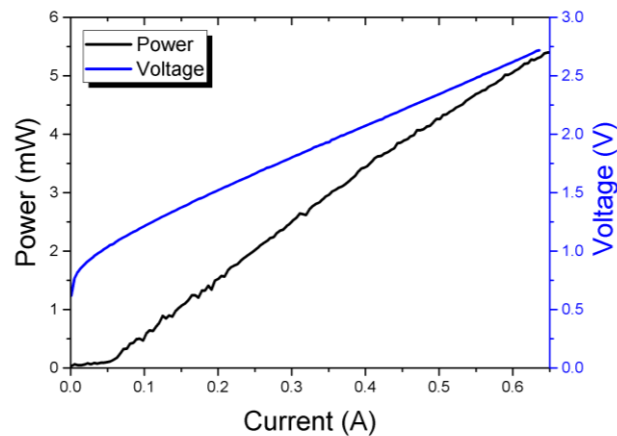
Figure 13: L-I-V characteristics of the chirped barrier thickness QDash LD under pulsed current operation at 14°C set by a heatsink.
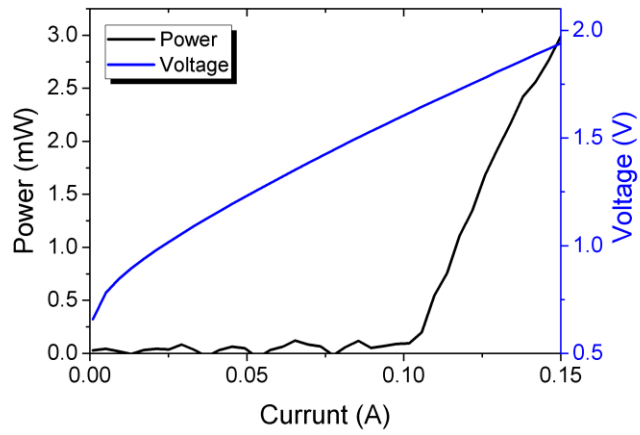
Figure 14: L-I-V characteristics of the chirped barrier thickness QDash LD under CW current operation at 14ºC.
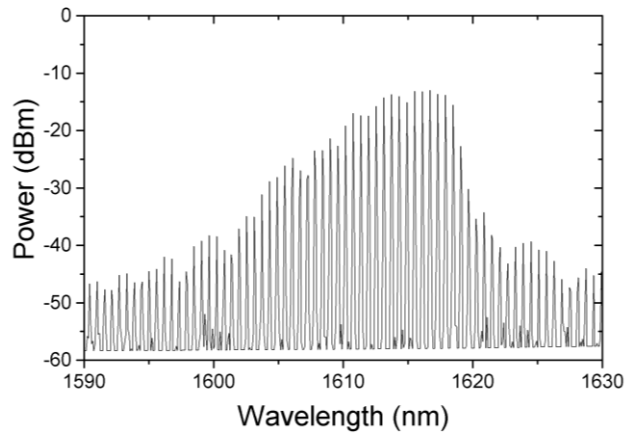
Figure 15: Free running lasing spectrum at 1.1 Ith for the 4×600 μm^2 cavity length chirped barrier QDash LD.

CHAPTER 3

SELF-INJECTION LOCKING CHARACTERIZATION

3.1   Introduction

In this chapter, self-injection locking of QDash LD is investigated thoroughly, by testing the stability and tunability of the lasing subcarrier besides controlling the number of active subcarriers. The chapter starts with a detail description of the setup utilized and then study the self-injection locking characteristics of one subcarrier in terms of stability, SMSR and tunability. Then, it demonstrates utilizing self-injection locked QDash LD as a selective multi-wavelength source.

3.2   Self-Injection Locking Experimental Setup

Fig. 16 shows the configuration of our self-injection locking experiment. The earlier characterized QDash LD was mounted on a brass base attached to two probes. The LD was biased at CW current mode using Kiethley 2520 Pulsed Laser Diode Test System, and kept at 14 °C using Kiethley TEC Source Meter. The QDash LD was butt coupled with a single mode fiber mount on a 3-D translational stage. Then, an L-band erbium doped fiber amplifier (EDFA) with a ~20 dB gain and a tunable band pass filter (BPF) with ~7 dB insertion loss were applied to the optical output of QDash LD in a feedback loop. The main rule of the amplifier is to compensate for the ~7 dB-filter loss and ~13 dB modulator and other coupling losses, and the BPF was employed to selectively filter out one single FP mode that will be re-injected into the QDash LD, thus self-injection locking one FP mode. A polarization controller was utilized to maximize the feedback power. A 3-dB coupler was used to divide the injection locked lasing power to be used

in self-injection locking and as a sub-carrier in optical communication. Then, an optical circulator (OC) was used to inject back the selected and amplified FP mode into the laser diode, and a polarization controller was directly applied to the LD terminal to maximize the feedback lasing power going into the laser diode. In the meanwhile, the amplified self-injection locked FP-LD subcarrier was observed via the OSA using 2:98% coupler.
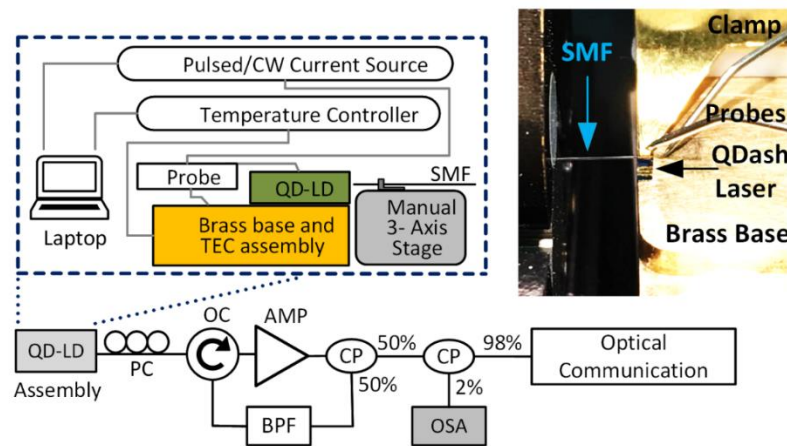
Figure 16: Self-injection locking experimental setup for QDash LD

3.3   Self-Injection Locked QDash LD as A Tunable Laser Source

By tuning the central wavelength and bandwidth of the BPF in the feedback loop to match only one FP mode, different FP modes in the range 1602-1613 nm were self-injection locked, however, by mismatching the passband with the FP mode, injection locking disappeared and free running is recovered as illustrated in Fig. 17(a). The self-injection locking resulted in a coherent laser source with at most 0.05-0.06 nm-FWHM (the resolution limit of our OSA) and ~18 tunable channels with 0.6 nm spacing to be utilized as subcarriers in the optical communication system. It is worth mentioning that this tuning range was only one half of the available tunable range, 1602-1630 nm given by the QDash LD, which could not be tested in our experiment due to the limitation of the amplifier operating band. Fig. 17 (b) shows that the total power (after the 3 dB-

coupler) and SMSR of the different self-injection locked FP modes were about ~9 dBm

and 30 dB, respectively, which corresponds to ~20 dB injection ratio (the self-injected

power to the free-running lasing power ratio at the laser facet) after calculating the

actual free running laser power and the self-injected power at that facet, assuming the

coupling ratio is the same in both directions. Although the injection ratio was very low,

self-injection locking of one single FP mode was performed due to self-feeding that

forced a resonation at that FP mode through enhancing stimulated emission.

Fig. 17 (c) shows the typical locking hysteresis, with width ~ 2dB, of the QDash LD at

1609.6 nm FP mode by increasing the mode power via varying the EDFA gain. An

abrupt increase in the SMSR from ~11dB to ~26 dB is observed by increasing the mode

power from ~5.5 to ~7dBm. Hence, this is the minimum mode power required to sustain

locking with the feedback configuration and corresponds to ~-22 dB injection ratio.
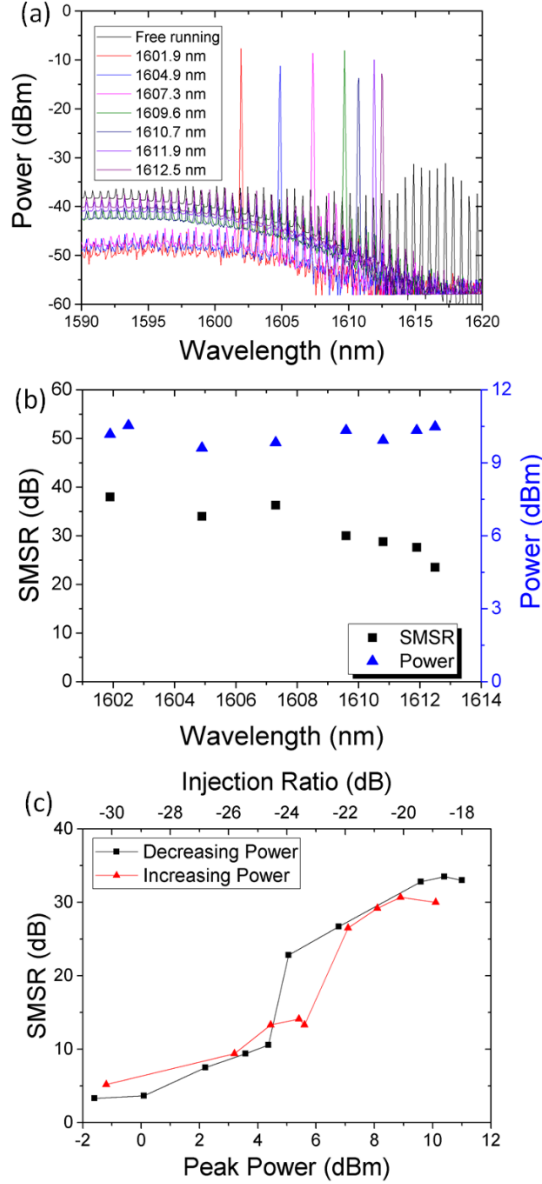
Figure 17: (a) Free running lasing spectrum and self-injection locking of different FP modes (measured at 2% coupler output) and (b) the corresponding integrated mode power (measured at 98% coupler output) and SMSR. (c) QDash LD hysteresis at 1609.6 nm locked mode.

Next, we systematically investigated the effect of locking behavior by comparing the short-term stability test of three different self-locked modes, 1603.2 (shorter wavelength edge of -25 dB lasing bandwidth), 1609.6 (longer wavelength edge of -8 dB lasing bandwidth) and 1613.2 (longer wavelength edge of -1.5 dB lasing bandwidth) nm over 20 min period, and the results are plotted in Fig. 18. Comparison across the figures indicated that the mode peak power and SMSR were more stable, within ± 0.1

dBm and ± 1 dB, respectively, for longer wavelength FP modes. In other words, locking is found to be more stable for the modes closer to central lasing wavelength of the QDash LD, in spite of smaller peak power and SMSR. This is attributed to appreciable contribution of coherent photons emitted in the QDash LD active region, taking part in the locking process compared to the incoherent ASE photons from EDFA. In fact, this ratio was the reason limiting us from blue shifting the self-locking wavelength tuning range. We found that below ~1612 nm, negligible contribution from QDash LD was observed due to the wavelength operation outside the -25 dB bandwidth. In general, all the three FP mode wavelength were also stable over the entire time period, thanks to the improvement of the QDash LD linewidth enhancement factor due to self-injection locking.
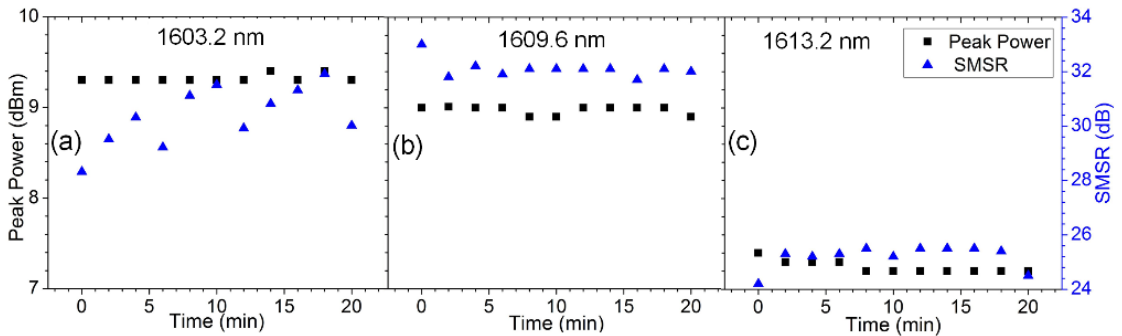
Figure 18: Short term stability test of the FP mode peak power and SMSR for different self-injection locked QDash FP modes at (a) 1603.2, (b) 1609.6, and (c) 1613.2 nm.

3.4   Self-Injection Locked QDash LD as a Multi-Wavelength Source

Figs. 19 (a-d) show the spectrum of the free running and the self-injection locking of different number of active Fabry Perot modes, performed through tuning the BPF bandwidth to control the number of FP modes fed back to the laser. Despite the self-injection FP modes number, the total lasing power was found to be constant at ~9 dBm at the 3-dB coupler output. Fig. 19 (e) shows the single subcarrier power (peak power) and SMSR for different number of self-injection locked FP modes between 1 and 16,

in the wavelength range 1600-1610 nm. However, self-injection locking can be extended to 1620 nm reaching up to 30 self-injection locked FP modes, however, we could not achieve due to the limitation of the EDFA amplifier operating band.
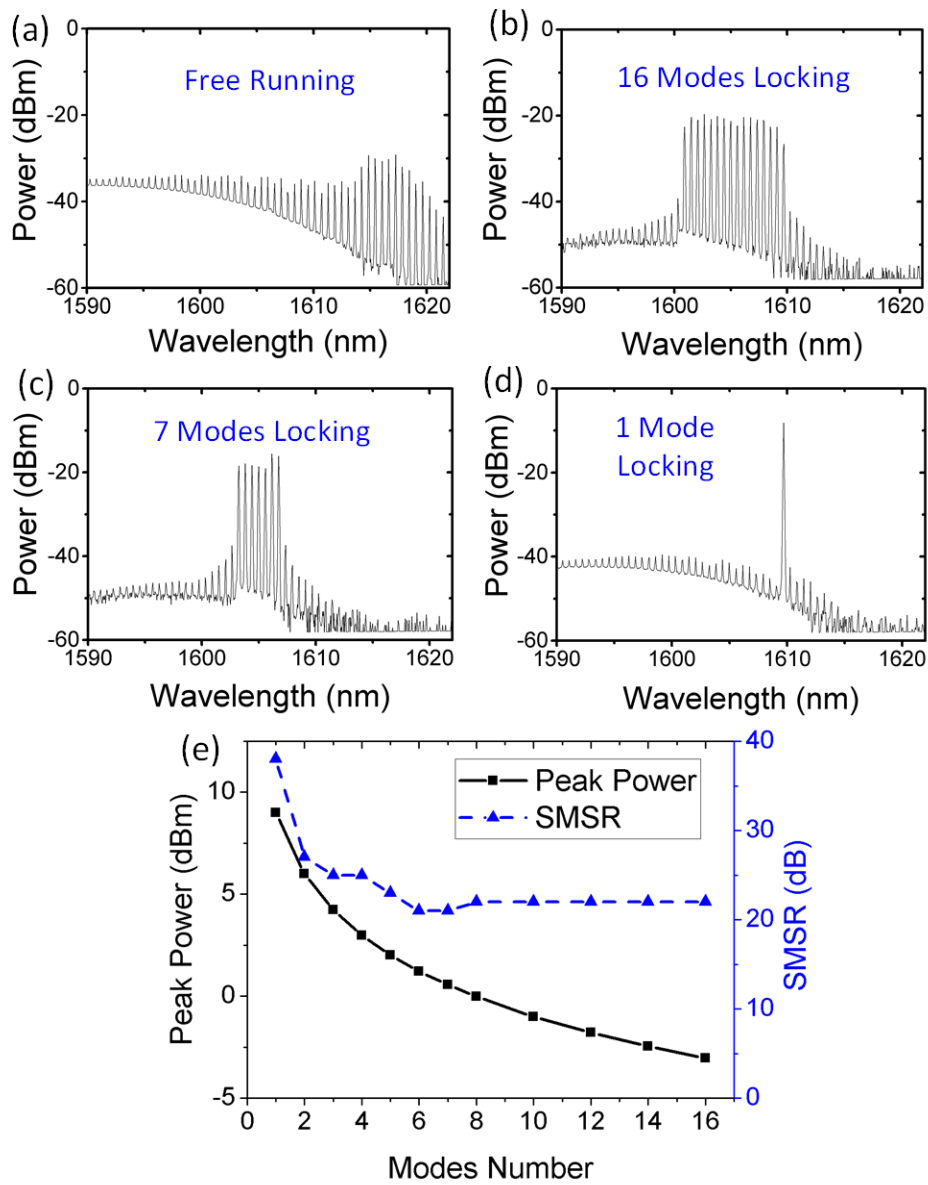
Figure 19: (a) Free running spectrum, (b-d) self-injection locking of different number of FP modes, and (e) the SMSR and single peak power versus the number of self-injection locked FP modes

CHAPTER 4

OPTICAL COMMUNICATION

4.1 Introduction

The self-injection locked QDash LD demonstrated in chapter 2 and 3 was utilized as a subcarrier generator for SMF and FSO coherent optical communication with DP-QPSK modulation scheme. The coherent communication was performed for different data rates at different received power. Then, we proposed a WDM-PON based on QDash LD as a multi-wavelength source.

4.2 Single Mode Fiber Communication

4.2.1 Experimental Setup

The self-injection locked mode at 1609.6 nm, shown in Fig. 17, with mode power ~9 dBm, was picked from the 98% end of the coupler and fed to the dual polarization in-phase quadrature external modulator (DP-IQM), as shown in Fig. 20. Pre-processing of the signal was performed using Matlab by generating pseudo random binary sequence (PRBS) with 2^{11}-1 length via an arbitrary wave generator (Keysight AWG M8195A) and mapped into quadrate phase shifting (QPSK) to obtained DP-QPSK format. The DP-QPSK modulation was performed using 64 Gbaud Linear Modulator (FTM7992HM) that consists of two QPSK modulators and polarization beam combiner and had 13 dB total insertion loss. The data transmission was characterized under back-to-back (BTB) and over 10 km or 20 km SMF, before being detected and analyzed by Keysight optical modulation analyzer (OMA-N4391A). A variable optical attenuator

(VOA) was utilized at the receiver end (before the OMA) to vary the power for BER versus received power measurement.
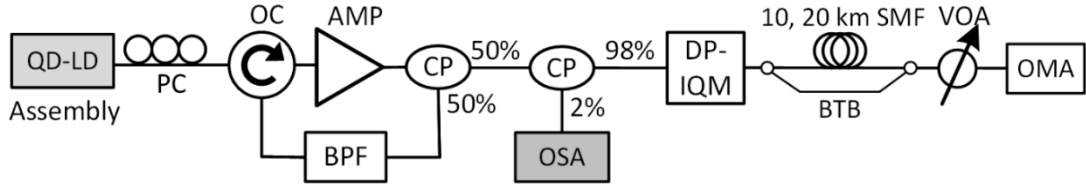
Figure 20: Utilization of self-injection locked QDash LD in SMF communication experimental setup

4.2.2 Optical Communication

Fig. 21(a) shows the transmission results of DP-QPSK scheme at 25 Gbaud (100 Gb/s), over 20 km SMF, utilizing 8 separate subcarriers (self-locked modes) from ~1602 – 1613 nm range. The measured bit error rate (BER) was found to be below FEC limit (3.8×10^{-3}) in all the cases at a stable received power at ~-11 dBm, after exhibiting ~13 (~7) dB modulator (BPF) losses, and the fiber loss of ~0.3 dB/km. The corresponding received clear constellation diagrams are shown in the inset of Fig. 21(a). These results demonstrate the feasibility of employing the proposed tunable L-band self-injection locked QDash LD as a promising source in next generation optical networks, in particular 100G NG-PONs. To test the capacity of the system, 1609.6 nm self-locked mode was selected as a subcarrier to transmit DP-QPSK signal at different data rates, from 32 Gbaud (128 Gb/s) to 48 Gbaud (192 Gb/s), utilizing various channels. Successful transmissions of 128 Gb/s over 20 km SMF and 168Gb/s over 10 km SMF were achieved with below FEC limit receiver sensitivities ~-15 dBm and ~-12.4 dBm, respectively. Fig. 21(b) shows the BER versus received power for these two cases, showing a power penalty of ~ 0.2 dB measured in the former case, the latter one exhibited a value of ~1.6 dB with a clear constellation diagram at received power of ~-10 dBm, shown in the inset of Fig. 21(b). Fig 22 (a) shows also the BER versus received

power at lower data rates 16 Gbaud (76 Gb/s)-20 km and 40 Gbaud (160 Gb/s)-10 km in comparison with BTB communication with power penalty of ~ 0 dBm and 1 dBm, respectively. Shown also are constellation and eye diagrams for both cases at a received power of ~ -10 dBm. Variation in the QDash LD coupled SMF power with time could be one plausible reason to the observation of minor difference in the receiver sensitivities of 128 Gb/s signal. Moreover, an effective transmission in the BTB configuration was achieved at 192 Gb/s data rate with receiver sensitivity ~-10 dB, however, via 10 km SMF resulted in BER > FEC limit. This is attributed partly to the larger linewidth (~0.06 nm) of the self-locked FP modes which could further be improved by applying high reflection coating on QDash LD facets. Hence, with the present wavelength tunability of >10 nm in the L-band, a single QDash LD is capable of achieving a capacity of > 3 Tb/s should all the self-locked modes be utilized simultaneously. It is worth mentioning that multiple modes could be self-locked by controlling the pass band of the BPF, thus exhibiting the characteristics of multi-wavelength laser as well as a tunable laser.
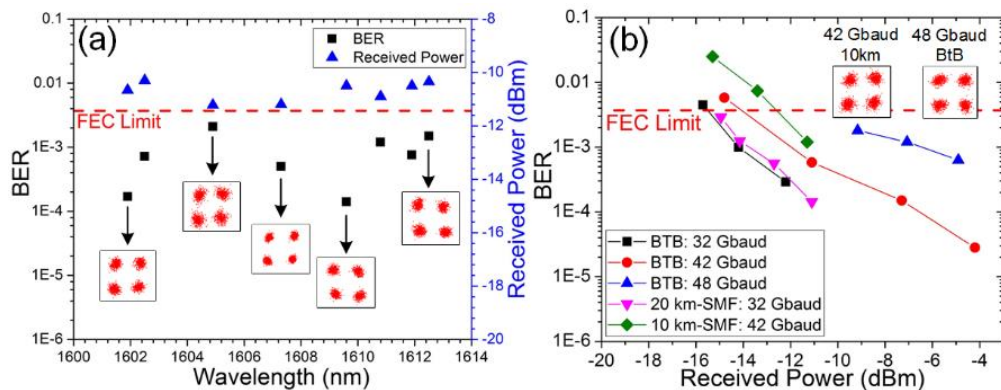
Figure 21: (a) Measured BER after 20 km SMF transmission of 100 Gb/s DP-QPSK signal utilizing different self-locked modes of QDash LD, covering the entire >10 nm tuning range. (b) Measured BERs versus the received power at different transmission data rates and channel lengths.
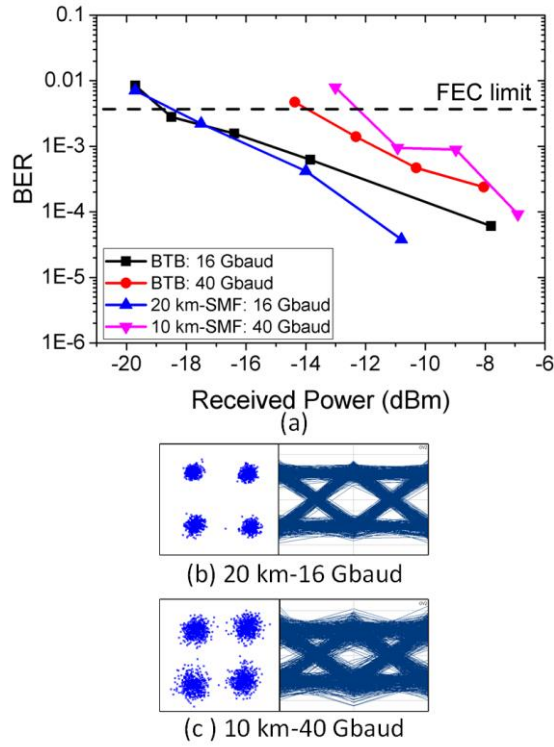
Figure 22: (a) Measured BER for 20 km SMF-16 Gbaud (64 Gb/s) and 10 km SMF-40 Gbaud (160 Gb/s) communication compared to BTB configuration, and (b, c) their constellation and eye diagrams, respectively.

4.2.3 WDM-PON Network Based on Self-Injection Locked QDash LD

In Fig. 23, we propose the multi subscribers WDM-PON based on a self-injection locked QDash LD as a unified down-streaming multi-wavelength source that would significantly reduce the system cost and simplify the design and implementation. The system is also employing single-wavelength self-injection locked QDash LD for upstreaming at the ONUs. The system can reach achieve a data capacity of 160 Gb/s with a BER below FEC limit subscriber and, thus, with the employment of the multi-subcarriers, it can achieve aggregate capacity of 1 Tb/s (16×16 Gbaud DP-QPSK) or 2.5 Tb/s (16×40 Gbaud DP-QPSK) over 20 km SMF channel. Table 3 shows the power budget of the proposed system, guaranteeing a power margin of 6 dB and 12 dB for 1

Tb/s (16×16 Gbaud DP-QPSK) and 2.5 Tb/s (16×40 Gbaud DP-QPSK) data capacity, respectively.

The proposed system has the capability of attaining any number of subscribers in WDM-PON between 1 and 16 with a unified design and maximum utilization of the lasing power performed through BPF tuning. Moreover, with the proper optimization and coupling (with 30 % coupling ratio) of the QDash-LD, and employing all of the available subcarriers 30, the stated data capacity reach higher values
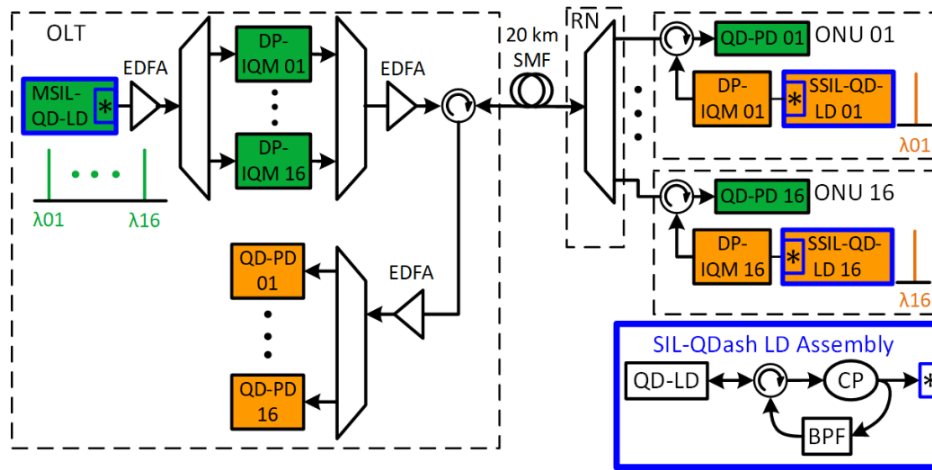
Figure 23: Proposed WDM-PON based on self-injection locked (SIL) QDash-LD as a multi wavelength. M(S)SIL-QD-LD stands for multi(single)-wavelength self-injection locked quantum dash LD.

Table 3: Power budget for proposed WDM-PON

Parameter	Downstream	Upstream
SIL-QDash LD single subcarrier power (dBm)	-3	9
Total EDFAs gain (dB)	31 (2 stages)	14 (1 stage)
Total AWGs loss (dB)	15 (3 stages)	10 (2 stages)
DP-IQM loss (dB)	13	
20 km SMF loss (dB)	6	6
Circulator and connectors losses	3	3
Receiver sensitivity (dBm)	-12 (40 Gbaud symbol rate)	
	-18 (16 Gbaud symbol rate)	
Power margin (dB)	3 (40 Gbaud symbol rate)	
	9 (16 Gbaud symbol rate)	

4.3 Free Space Optical Communication

4.3.1 Experimental Setup for FSO Communication

The experimental setup for the free space communication is shown in Fig. 24, which is similar to that utilized for the fiber transmission (Fig. 20), except the channel is now free space. The FSO channel is implemented indoor using two collimated SMF and a mirror before it was coherently detected using an optical modulation analyser. An attenuator was utilized before the OMA to vary the received power to study BER versus received power for the specific communication channel.
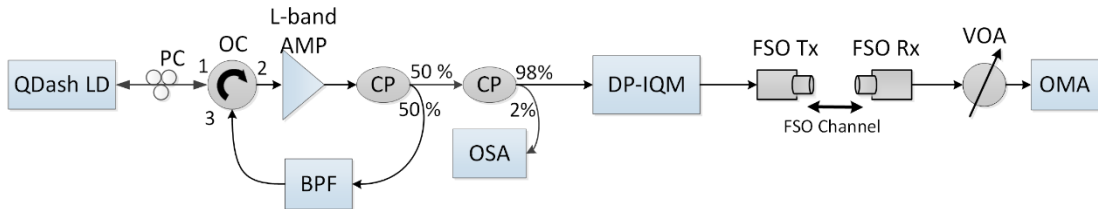
Figure 24: Self-injection locking arrangement and the transmission setup showing the FSO channel.

4.3.2 Optical Communication

The self-injection locked FP mode was utilized as a subcarrier to transmit a pseudo random binary sequence with different data rates through 16 m FSO channel. The tunability of self-injection locking was studied for four different FP modes in the range 1603-1610 nm which consists of 12 tunable subcarriers, shown in Fig. 25(a), with ~9 dBm peak power, ~30 dB SMSR and ~ 0.05 nm FWHM. Then, these self-injection locked subcarriers were utilized to transmit 32 Gbaud signal through 16 m FSO channel with received BER below FEC limit, as shown in Fig. 25(b). The results showed that the transmission performance degraded for the 1610.8 nm FP mode due to the reduction in SMSR due to approaching the weak amplification band and, thus, weaker injection ratio. Then, the self-injection locked 1609.7 nm FP mode was utilized as a subcarrier

for FSO communication with different symbol rates, 16, 32, 40 and 44 Gbaud (64, 128, 160 and 176 Gb/s) and 16 m channel distance. The power loss due to the 16 m FSO channel was estimated to be 8 dB, as measured at the receiver terminal with 0 dB attenuation. Fig. 25(c) shows the BER versus received power, achieved through varying the attenuation, when compared with BTB configuration, showing a receiver sensitivty of -18.2, -17.5, -16.0 and -15.5 dB, respectively. Fig. 25(d) shows the variation in the BER and received power due to introducing a misalignment in the transmitter for 1609.7 nm subcarrier and 32 Gbaud (128 Gb/s) signal through 16 m FSO channel. Up to ~2.5 mm misalignment could be tolerated by the channel without loss of the transmission.
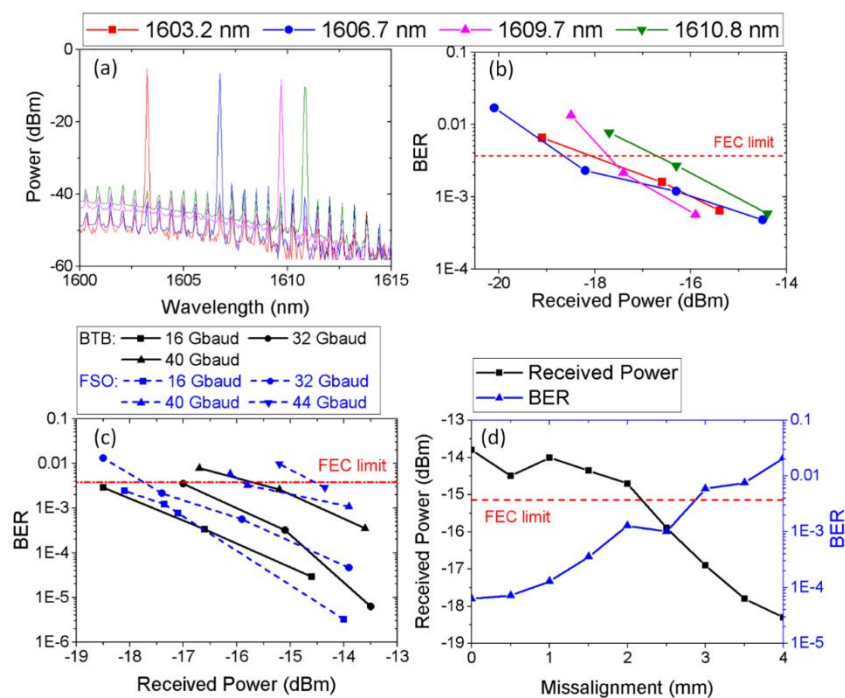
Figure 25: (a) the optical spectrum of different self-injection locked FP modes, (b) the measured BER versus received power for three self-injection locked FP modes at 32Gbaud and 16 m FSO link, (c) BER versus received power for transmission through BTB configuration and 16 m FSO channel at 1609.7nm and (d) measured BER and received power while introducing a misalignment in the transmitter at 1609.7 nm

In addition, the 1606.7 nm self-injection locked FP mode was utilized as a subcarrier to transmit 32 Gbaud (128 Gb/s) and 44 Gbaud (176 Gb/s) pseudo random binary

sequence through FSO channel. The impact of the injection ratio on the side mode suppression ratio (SMSR) and the transmission performance for 5 m FSO channel that have a channel loss of 4.5 dB was studied through varying the peak power, resulting in an SMSR = ~30 dB and BER = ~10^{-5} for injection ratio = -20 dB and peak power = 10 dBm, as shown in Fig. 26(a). Thus, a minimum injection ratio of ~ -20 dBm was required to maintain self-injection locking. Fig. 26(b) shows the BER versus received power for the 1606.7 nm self-injection locked subcarrier used for 5 m FSO communication for different channel distances, for 32 Gbaud symbol rate (128 Gb/s) with a receiver sensitivity of -16 dBm. Shown also the constellation diagrams for at the different received power. However, the BER measured for 5 m FSO communication was higher than the BER measured for 16 m FSO communication in spite of the expectation, as the polarization controller was not fully optimized for maximum injection ratio that affected the self-injection locked QDash LD coherency, resulting in lower SMSR values and, thus, the communication performance.
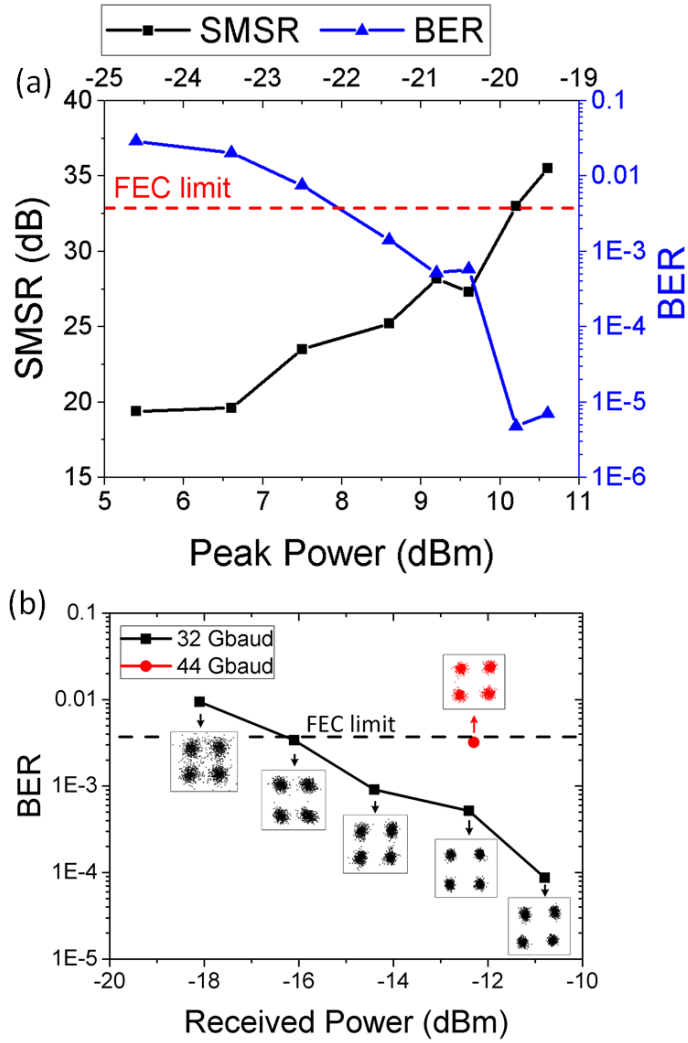
Figure 26: (a) measured SMSR and BER while varying the injection ratio and the self-injected peak power (b) BER versus received power for 5 m FSO communication and 32 Gbaud and 44 Gbaud symbol rate for 1606.7 nm FP mode utilized as a sub-carrier, shown also are the constellation diagrams at different received power.

CHAPTER 5

INJECTION LOCKED BLUE INGAN/GAN LASER

DIODE

5.1   Introduction

In this chapter, we characterized the external injection locking of blue InGaN/GaN commercially available LD focusing on the locked mode stability, and minimum master laser power. Later, we demonstrate a VLC based on the injection locked blue LD using OOK modulation scheme up to 2 Gb/s..

5.2   Experimental Setup

External injection locking was investigated for blue semiconductor LD using the schematic diagram and experimental setup shown in Figs. 27, and 28, respectively. Two commercially available single mode blue InGaN/GaN LDs (Thorlabs PL450B) shown in Fig. 29, were utilized as a master and slave source. The two LD were mounted on a Thermoelectric Cooler (TEC) integrated mount (LDM9T) controlled with an external controller (Thorlabs ITC4001). Two convex lenses were used to collimate the beams from the two LD sources. Then, the master source was directed toward the slave LD for external injection locking. In the meanwhile, a 92/8 % beam splitter (BS) was utilized to monitor the slave laser lasing spectrum at the 8% output while the 92% output was utilized to pass the master LD into the slave LD. Then, a 50/50% BS was utilized to split the slave LD power to be monitored using an optical spectrum analyzer (OSA) and transmitted over a 20 cm free space optical channel to be detected using a

photo-detector (Montosystems APD 210). The modulation bandwidth of the laser diode was measured using a network analyzer (Agilent Technologies E8361C). Then, the slave laser diode was directly modulated with OOK scheme generated using an RF signal generator (Agilent Technologies N4903B). and, the received signal was analyzed using a digital communication analyzer (Agilent DCA-J 86100C) and a high-performance bit error rate tester (Agilent J-BERT N4903B).
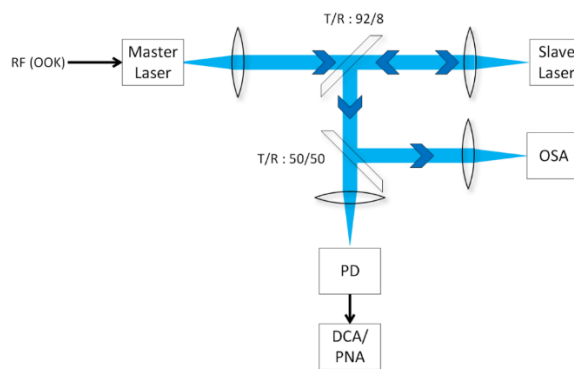
Figure 27: The schematic diagram of the free space external injection locking utilized in the work for the blue InGaN/GaN laser diode
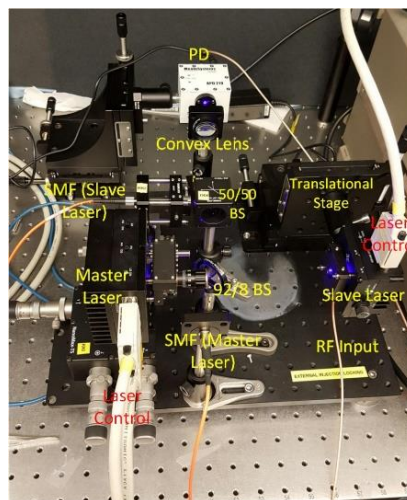
Figure 28: The experimental setup of the free-space external injection locking utilized in the work for the blue InGaN/GaN laser diode

41

Figure 29: Commercial InGaN/GaN blue LD [52].

5.3 External Injection Locking Characterization

5.3.1 L-I-V Characterization of Blue LD

The L-I-V characteristics of the blue LD are shown in Fig. 30, with a threshold current I_{th} of 50 mA, at room temperature. The LD biasing current and temperature were controlled to fine tune the central lasing wavelength. Then, two blue LD were utilized as a master and slave LD sources in ijnetion locking experiment with the specifications given in Table 4.
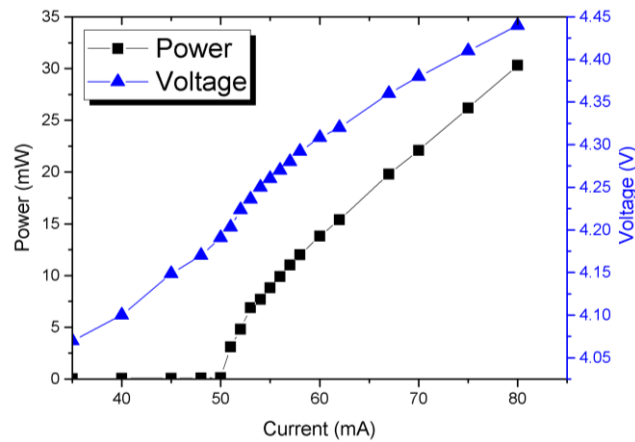
Figure 30: L-I-V Characteristics of blue laser diode

Table 4: InGaN/GaN blue master and slave laser diode characteristics

Laser source	Wavelength (nm)	Operation current (A)	Temperature (℃)	Total power (mW)
Master laser	450.5	0.048	20	12
Slave laser	452.0	0.054	25	14

5.3.2   Spectral Analysis of Injection Locking

Fig. 31 shows the master laser spectrum at 20°C to be centred at 450.5 nm, that is blue shifted by 1.5 nm compared to the free running spectrum of the slave laser centred at 452.0 nm and set at 25°C, shown in Fig. 32. Fig. 32, shows also the comparison between the free running and injection locked spectrum. We observed that the peak power of the slave laser almost doubled after injection locking while the total power stayed the same. In the meanwhile, the side mode suppression ratio (SMSR) has increased substantially from 2-3 dB to 8-10 dB due to injection locking, producing more coherent lasing spectrum. However, almost no change was observed in the central lasing wavelength and the total lasing power.
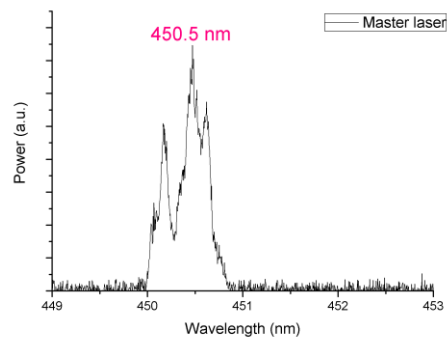
Figure 31: The lasing spectrum of the master laser
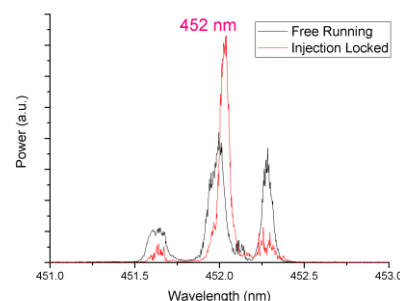
Figure 32: Free running and the injection locked lasing spectrum of the slave laser

However, by increasing the temperature of master laser source from 20 °C to 30 °C and 35°C, the master laser spectrum was shifted to 451.1 nm and 451.5 nm, respectively,

which matches the lasing spectrum of the slave laser. However, the injection locked lasing spectrum showed similar behavior to previous case (25℃, 450.5 nm) in terms of the peak power, total power and SMSR.

5.3.3 Time Analysis

Fig. 33 shows the injection locking evolution of the slave laser spectrum after injection locking i.e. once the master laser is turned on, showing that about 3 minutes was required to maintain high coherency, i.e. single FP peak. Fig. 34 shows the corresponding change in SMSR over time, showing high fluctuation in injection locking in the first 3 min before stabilizing after 4 min. However, this settling time would be only required when initiating the laser diode, and, then, it would remain stable for continuous operation, that is the case required in communication system. Thus, in our experiment, a period of 5 minutes was provided for injection locking to stabilize before any further analysis. Then, the stability of the injection locked slave laser diode mode was performed showing a stable single mode peak in most of the instances with an average SMSR value of in the range 8-10 dB, as shown in Fig. 35. However, slight decrease was observed in the SMSR value at one instance due to the difficulty in keeping perfect alignment i.e. coupling master laser power into the slave laser since its emitting surface had a very small size of 0.2 mm × 0.1 mm as measured with using a microscope. However, in order to improve injection locking stability better coupling with sensitive may be needed.
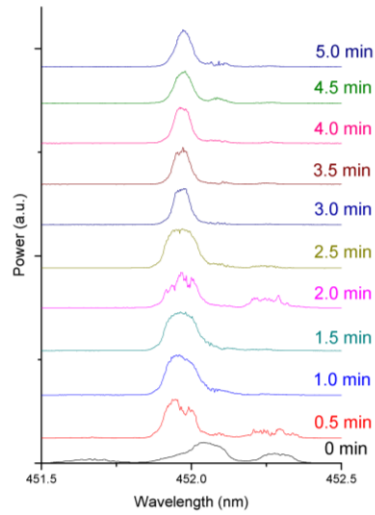
Figure 33: Stability analysis of the locked slave laser mode just after turning on the master laser source.
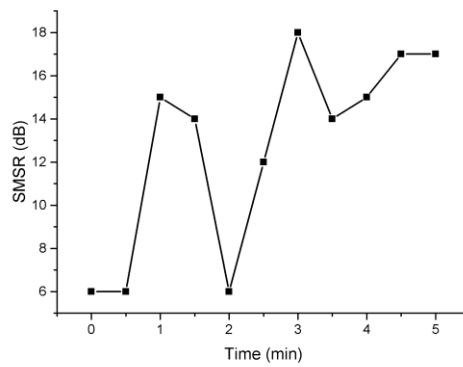
Figure 34: SMSR of the slave laser after turning the master laser source on.
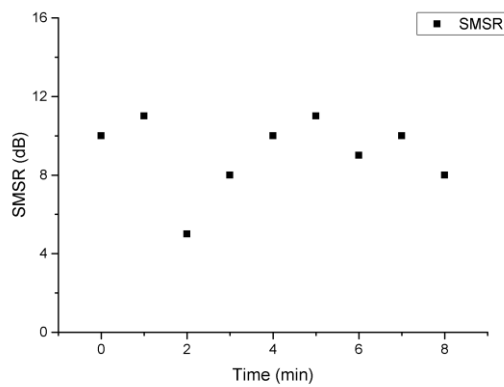
Figure 35: Stability test of the injection locked spectrum after providing 5 min stabilization time to the locked mode.

5.3.4 Dependence of Master LD Power or the Injection Ratio

Fig. 36 shows the effect of changing the master LD power over the injection locking behavior of the slave LD spectrum, and Fig. 37 shows the corresponding SMSR of the locked mode at different master laser power, showing a significant increase in the SMSR for a master laser power bigger than 4 dBm, that is the minimum master laser power required to maintain injection locking. However, due to the difficulty in coupling the master laser power into the slave laser, the SMSR value fluctuated as the master laser power exceeded 4 dBm, which should not be the case, rather it was expected to remain stable in spite of the master laser power.
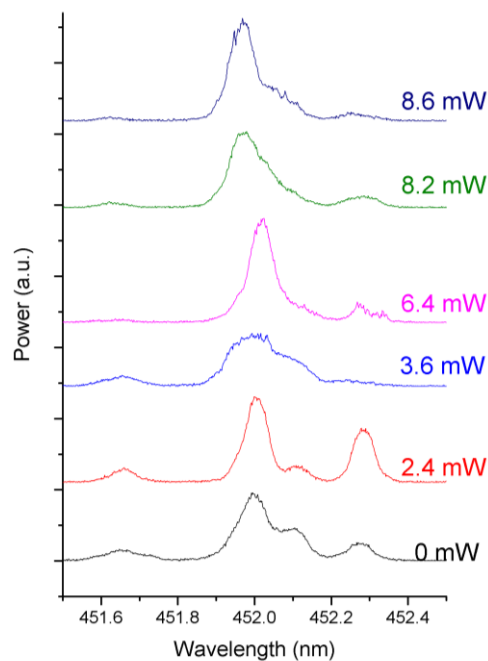
Figure 36: Slave laser spectrum at different master laser power
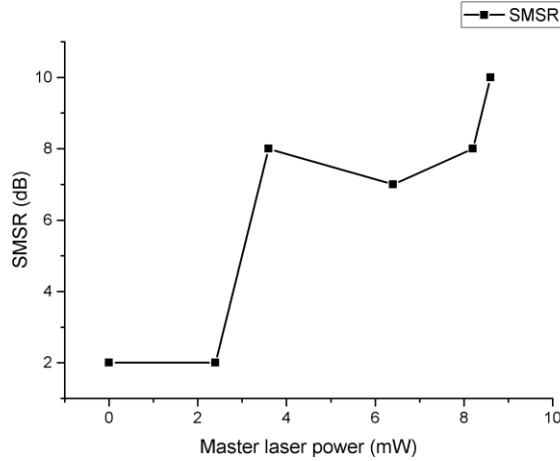
Figure 37: SMSR of the slave laser at different master laser power

5.4   Optical Communication

Fig. 38 shows the frequency response in terms of transmission coefficient S21, that is the RF received power in APD to the power transferred to the laser diode, for the free running slave blue LD showing a cut-off frequency at 1.0 GHz. However, no marked difference in the cut-off frequency was observed between free running and injection locked. Then, OOK communication was performed for the free running slave LD at different data rates and the received BER was measured, as shown in Fig. 39, showing a BER $\leq 10^{-8}$ (device limitation) for data rates ≤ 1.5 Gb/s and a successful transmission up to 2.1 Gb/s with BER < FEC limit, that is around twice the cut-off frequency 1 GHz. Also, the received eye diagrams are shown in Figs. 40 (a-g) for different data rates showing an open eye for data rates ≤ 2.1 Gb/s. However, no marked difference was observed in the cut-off frequency nor BER nor data rates between injection locking and free running cases, which is attributed to the fact that the total lasing power stayed constant. However, a laser mount with higher cut-off frequency must be employed, in order to increase the transmission capacity or lower BER.
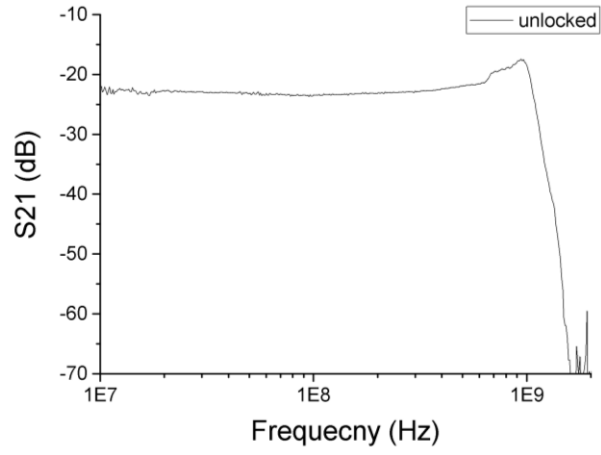
Figure 38: Frequency response of the slave laser diode in free running case.
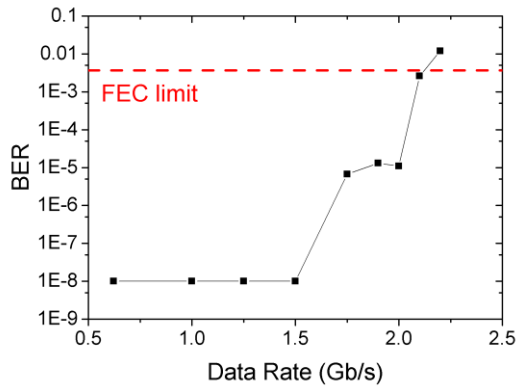
Figure 39: Measured BER at different OOK data rates

(a) 0.625 Gb/s

(b) 1.25 Gb/s

(b) 1.5 Gb/s

(d) 1.75 Gb/s

(e) 1.8 Gb/s

(f) 2 Gb/s

(g) 2.1 Gb/s

(h) 2.2 Gb/s
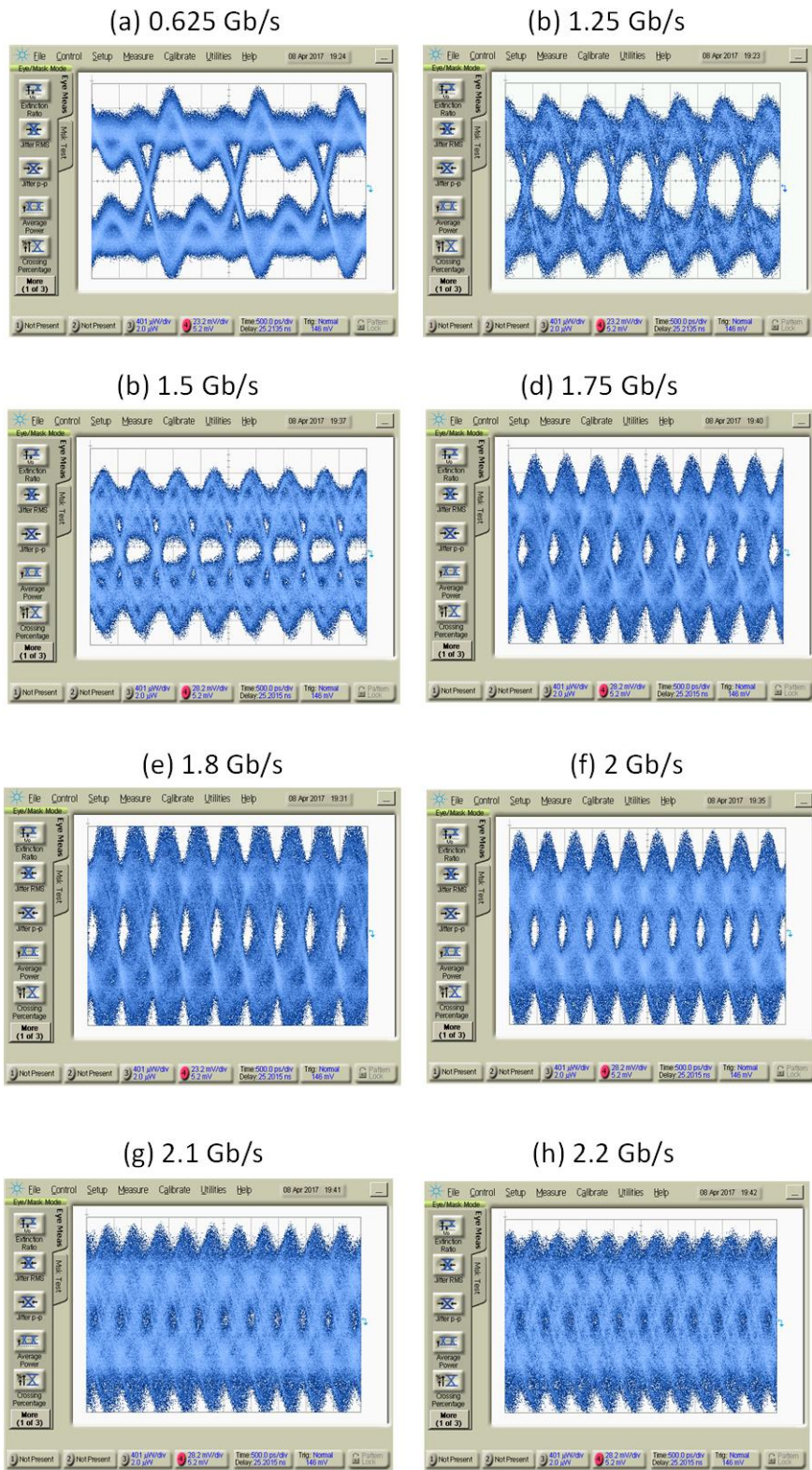
Figure 40 (a-h): Measured eye diagram at different data rates

CHAPTER 6

CONCLUSION AND FUTURE WORK

6.1 Conclusion

The performance variation between the two fixed barriers QDash LDs structures with dash elongation being parallel and perpendicular to the laser cavity facet, in terms of efficiency, internal loss and center wavelength, were discussed. It was found that the chirped barrier thickness device structure displayed superior performance and was working in CW mode with a lasing band at the far L-band, ~1600 to 1620 nm.

We investigated self-injection locked L – band QDash LD as a tunable single subcarrier with focus on mode power, SMSR, short-term stability, and tunability. Promising results has been reported with > 10 nm tunability (1602 – 1613 nm) with stable > 28 dB SMSR. Then, we demonstrated an L-band multi-wavelength source based on self-injection locked QDash LD with a controllable number of active subcarriers between 1 and 16. Next, separate self-injection locked FP modes were utilized as subcarriers to achieve 100 Gb/s DP-QPSK transmission via 20 km SMF in the entire tuning wavelength range. Besides, their potential to achieve > 168 Gb/s transmission is demonstrated via successful transmission (channels) of up to 192 Gb/s (BTB), 168 Gb/s (10 km SMF) and 128 Gb/s (20 km SMF) DP-QPSK signals. The deployment of such a source in WDM-PONs, potentially providing an aggregate capacity of > 3Tb/s in far L–band, would enable cost-effect unified transmitters serving multi subscribers, while addressing the expanded spectrum wavelength plan of NG-PONs beyond C – band. Finally, we proposed 1 Tb/s (16×16 Gbaud DP-QPSK)-20 km and 2.6 Tb/s (16×40

Gbaud DP-QPSK)-20 km multi-subscribers WDM-PON using multi-wavelength source and single-wavelength self-injection locked QDash LD for downstreaming and upstreaming, respectively, that would significantly reduce the system cost and simplify the design and implementation.

Moreover, tunable self-injection locked QDash LD was also demonstrated as a subcarrier for L-band FSO communication. FSO communication with different symbol rates was demonstrated with up to 16 m-176 Gb/s FSO communication performed with BER below FEC. In addition, the impact of injection ratio, transmitter-receiver misalignment was investigated.

Finally, external injection locking of blue LD was investigated with focus on laser coherency (SMSR), stability and master laser power. In addition, VLC communication based on direct modulated blue LD was demonstrated with up to 2 Gb/s data rate with OOK modulation scheme.

6.2   Future Work

- Optical communication based on self-injection locked QDash LD can be extended for outdoor FSO communication to be extended for more future application. Also, optical communication based on self-injection locked QDash LD can be generalized for SMF-FSO hybrid channels to easily link different types of environment. Also, higher order of modulation schemes such as 16 QAM can be looked at, but still better optimization of QDash LD growth and improving laser-fiber coupling is needed to achieve such a scheme.

- More investigation could be done on the multi-wavelength self-injection locked to test how the number of active subcarriers would change on the channel

performance, which could not be achieved in our work due to the limitation in equipment.

- In VLC, better bandwidth efficient modulation schemes such as OFDM or DTM can be utilized to boost the data rate to more than 4 Gb/s. Also, external modulation is another solution that can boost the optical communication data rates to overcome the limitation on modulation bandwidth caused by LD slow response.

Bibliography

[1]   W. Paper, "Cisco Visual Networking Index:Forcast and Methadology, 2015–2020", *Tech. Rep* 2016.

[2]   D. Nesset, "PON Roadmap [Invited]," *Journal of Optical Communications and Networking,* vol. 9, no. 1, pp. 71–76, 2017.

[3]   F. Wdm-pon, W. D. M. T. Systems, J. Kani, and I. Paper, "Enabling Technologies for Future Scalable and flexible WDM-PON and WDM/TDM-PON systems." *IEEE Journal of Selected Topics in Quantum Electronics,* vol. 16, no. 5, pp. 1290–1297, 2010.

[4]   K. Y. Cho, S. Member, U. H. Hong, S. Member, M. Suzuki, and Y. C. Chung, "103-Gb / s Long-Reach WDM PON Implemented by Using Directly Modulated RSOAs," *IEEE Photonics Technology Letters*, vol. 24, no. 3, pp. 2011–2013, 2012.

[5]   E. K. Machale, G. Talli, P. D. Townsend, A. Borghesani, and I. Lealman, "Extended-Reach PON Employing 10Gb / s Integrated Reflective EAM-SOA." *Optical Communication, ECOC, 34th European Conference.* IEEE, vol. 4, no. September, pp. 115–117, 2008.

[6]   D. Transmission, M. Cheng, C. Tsai, S. Member, and Y. Chi, "Direct QAM-OFDM Encoding of an L-band master-to-slave injection-locked WRC-FPLD pair for 28× 20 Gb/s DWDM-PON transmission," *Journal of Lightwave Technology,* vol. 32, no. 17, pp. 2981–2988, 2014.

[7]   L. Joulaud, C. Paranthoen, A. Le Corre, N. Bertru, H. Folliot, P. Caroff, and S. Loualiche, "InAs self-assembled quantum dot and quantum dash lasers on InP for 1.55 μm optical telecommunications." Information and Communication Technologies, vol. 2, pp. 2085-2090. 2006.

[8]   M. Zahed, M. Khan, T. K. Ng, C. Lee, P. Bhattacharya, B. S. Ooi, and S. Member, "Investigation of Chirped InAs / InGaAlAs / InP Quantum Dash Lasers as Broadband Emitters," *IEEE Journal of Quantum Electronics*, vol. 50, no. 2, pp. 51–61, 2014.

[9]   P. Ridha, L. Li, A. Fiore, G. Patriarche, M. Mexis, P. M. Smowton, P. Ridha, L. Li, A. Fiore, and G. Patriarche, "Polarization dependence study of electroluminescence and absorption from In As / Ga As columnar quantum dots Polarization dependence study of electroluminescence and absorption from InAs / GaAs columnar quantum dots," *Applied Physics Letters,* vol. 91, no 19, 2007.

[10]   S. Hein, P. Podemski, G. Sęk, J. Misiewicz, P. Ridha, A. Fiore, G. Patriarche, S. Höfling, A. Forchel, S. Hein, P. Podemski, G. S. J, J. Misiewicz, P. Ridha, A. Fiore, and G. Patriarche, "Orientation dependent emission properties of columnar quantum dash laser structures Orientation dependent emission properties of columnar quantum dash," *Applied Physics Letters,* vol. 94, no. 24, pp. 4–7, 2009.

[11] A. J. Zilkie, J. Meier, P. W. E. Smith, M. Mojahedi, J. S. Aitchison, P. J. Poole, C. N. Allen, P. Barrios, and D. Poitras, "Femtosecond gain and index dynamics in an InAs / InGaAsP quantum dot amplifier operating at 1 . 55 μm," *Optics express,* vol. 14, no. 23, pp. 11453–11459, 2006.

[12] T. Akiyama, M. Ekawa, M. Sugawara, K. Kawaguchi, H. Sudo, A. Kuramata, H. Ebe, and Y. Arakawa, "An Ultrawide-Band Semiconductor Optical Amplifier Having an Extremely High Penalty-Free Output Power of 23 dBm Achieved With Quantum Dots," *IEEE Photonics Technology Letters,* vol. 17, no. 8, pp. 1614–1616, 2005.

[13] U. Koren, B. I. Miller, Y. K. Su, T. L. Koch, and J. E. Bowers, "Low internal loss separate confinement heterostructure InGaAs/InGaAsP quantum well laser," *Applied physics letters*, vol. 1744, no. 1987, pp. 5–8, 1989.

[14] R. D. Dupuis, P. D. Dapkus, N. H. Jr, E. A. Rezek, R. Chin, A. D. Dupuis, and P. D. Dapkus, "Room - temperature laser operation of quantum - well Ga (1 − x) Al x As - GaAs laser diodes grown by metalorganic chemical vapor deposition Room-temperature laser operation of quantum-well Ga (1 _ x) AlxAs-GaAs laser diodes grown by metalorganic chemical vapor depositional," *Applied Physics Letters*, vol. 295, no. 1978, 1990.

[15] R. H. Wang, A. Stintz, P. M. Varangis, T. C. Newell, H. Li, K. J. Malloy, and L. F. Lester, "Room-Temperature Operation of InAs Quantum-Dash Lasers on InP (001)," *IEEE Photonics Technology Letters*, vol. 13, no. 8, pp. 767–769, 2001.

[16] R. Schwertberger, D. Gold, J. P. Reithmaier, and A. Forchel, "Long-Wavelength InP-Based Quantum-Dash Lasers," *Photonics Technology Letters*, vol. 14, no. 6, pp. 735–737, 2002.

[17] J. Pfeifle, I. Shkarban, S. Wolf, J. N. Kemal, C. Weimann, W. Hartmann, N. Chimot, and S. Joshi, "Coherent Terabit Communications Using a Quantum - Dash Mode - Locked Laser and Self - Homodyne Detection," *Optical Fiber Communications Conference and Exhibition (OFC)* pp. 6–8, 2015.

[18] A. Somers, W. Kaiser, J. P. Reithmaier, and A. Forchel, "InP-based quantum dash lasers for broadband optical amplification and gas sensing applications," *Indium Phosphide and Related Materials,* pp. 85–88, 2005.

[19] Q. T. Nguyen, L. Bramerie, G. Girault, O. Vaudel, P. Besnard, J. Simon, A. Shen, G. H. Duan, and C. Kazmierski, "16x2 . 5 Gbit / s Downstream Transmission in Colorless WDM-PON based on Injection-Locked Fabry-Perot Laser Diode using a single Quantum Dash mode-locked Fabry- Perot laser as multi-wavelength seeding source," *Optical Fiber Communication Conference. Optical Society of America,* pp. 9–11, 2009.

[20] M. T. A. Khan, E. Alkhazraji, A. M. Ragheb, H. Fathallah, S. Member, S. Alshebeili, and M. Z. M. Khan, "100 Gb / s Single Channel Transmission Using Injection-locked 1621 nm Quantum-dash Laser," *IEEE Photonics Technology Letters*, vol. 29, no. 6, pp. 543-546, 2017.

[21] R. Watts, R. Rosales, F. Lelarge, A. Ramdane, and L. Barry, "Mode coherence measurements across a 1 . 5 THz spectral bandwidth of a passively mode-locked

quantum dash laser," *Optics Letters*, vol. 37, no. 9, pp. 1499–1501, 2012.

[22] T. Habruseva, S. O. Donoghue, N. Rebrova, F. Kéfélian, S. P. Hegarty, and G. Huyet, "Optical linewidth of a passively mode-locked semiconductor laser," *Optics letters*, vol. 34, no. 21, pp. 1499–1501, 2012.

[23] R. Maher, K. Shi, L. P. Barry, J. Carroll, B. Kelly, R. Phelan, J. O. Gorman, and P. M. Anandarajah, "Implementation of a cost-effective optical comb source in a WDM-PON with 10 . 7Gb / s data to each ONU and 50km reach," Optics Express, vol. 18, no. 15, pp. 15672–15681, 2010.

[24] J. N. Kemal, V. Panapakkam, P. Trocha, and S. Wolf, "WDM Transmission Using Quantum-Dash Mode-Locked Laser Diodes as Multi-Wavelength Source and Local Oscillator," *Optical Fiber Communication Conference. Optical Society of America*, 2017.

[25] J. N. Kemal, K. Merghem, G. Aubin, and C. Calo, "32QAM WDM Transmission Using a Quantum-Dash Passively Mode-Locked Laser with Resonant Feedback," *Optical Fiber Communication Conference. Optical Society of America*, vol. 1, no. d, pp. 7–9, 2017.

[26] H. Lee, H. Cho, J. Kim, and C. Lee, "A WDM-PON with an 80 Gb / s capacity based on wavelength-locked Fabry-Perot laser diode," Optics Express, vol. 18, no. 17, pp. 18077–18085, 2010.

[27] C. Yeh, C. Chow, S. Member, Y. Wu, and S. Huang, "Performance of Long-Reach Passive Access Networks Using Injection-Locked Fabry – Perot Laser Diodes With Finite Front-Facet Re fl ectivities," *Journal of Lightwave Technology*, vol. 31, no. 12, pp. 1929–1934, 2013.

[28] C. Yeh and C. Chow, "Optical Fiber Technology Wavelength-selectable single-longitudinal-mode Fabry – Perot laser source using inter-injection mode-locked technique," *Opt. Fiber Technol.*, vol. 16, no. 5, pp. 271–273, 2010.

[29] C. H. Yeh, C. W. Chow, H. Y. Chen, J. Y. Sung, and Y. L. Liu, "Demonstration of using injection-locked ´rot laser diode for 10 Gbit / s 16-QAM OFDM WDM-PON," *Electronics letters*, vol. 48, no. 15, pp. 15–16, 2012.

[30] Z. Xu, Y. Yeo, X. Cheng, and E. Kurniawan, "20-Gb / s Injection Locked FP-LD in a Wavelength-Division- Multiplexing OFDM-PON," *Optical Fiber Communication Conference and Exposition (OFC/NFOEC)*, pp. 51–53, 2012.

[31] C. Tseng, C. Liu, J. Jou, W. Lin, C. Shih, S. Lin, S. Lee, S. Member, and G. Keiser, "Bidirectional Transmission Using Tunable Fiber Lasers and Injection-Locked Fabry – Pérot Laser Diodes for WDM Access Networks," *IEEE Photonics Technology Letters*, vol. 20, no. 10, pp. 794–796, 2008.

[32] E. Wong, K. L. Lee, and T. B. Anderson, "Directly Modulated Self-Seeding Reflective Semiconductor Optical Amplifiers as Colorless Transmitters in Wavelength Division Multiplexed Passive Optical Networks," *Journal of Lightwave Technology*, vol. 25, no. 1, pp. 67–74, 2007.

[33] M. Presi, A. Chiuchiarelli, R. Corsini, and E. Ciaramella, "Uncooled and

Polarization Independent Operation of Self-Seeded Fabry – Pérot Lasers for WDM-PONs," *IEEE Photonics Technology Letters*, vol. 24, no. 17, pp. 1523–1526, 2012.

[34]   F. Yuan, C. Hung, C. Wai, C. Hsuan, and S. Chi, "Optical Fiber Technology Utilization of self-injection Fabry – Perot laser diode for long-reach WDM-PON," *Opt. Fiber Technol.*, vol. 16, no. 1, pp. 46–49, 2010.

[35]   C. H. Yeh, C. W. Chow, Y. F. Wu, F. Y. Shih, and S. Chi, "Using Fabry-Perot laser diode and re fl ective semiconductor optical ampli fi er for long reach WDM-PON system RN," *Optics Communications*, vol. 284, pp. 5148–5152, 2011.

[36]   T. Komljenovic, D. Babic, and Z. Sipus, "C and L band Self-seeded WDM-PON Links using Injection- locked Fabry-Pérot Lasers and Modulation Averaging," *Optical Fiber Communications Conference and Exhibition (OFC),* pp. 14–16, 2014.

[37]   S. Hann and C. Park, "Upstream signal transmission using a self-injection locked Fabry-Perot laser diode for WDM-PON," *Optical Engineering*, vol. 44, no. June 2005, pp. 5–6, 2015.

[38]   J. Ramón, D. Retamal, H. M. Oubei, B. Janjua, Y. Chi, H. Wang, C. Tsai, T. K. Ng, D. Hsieh, M. Alouini, J. He, G. Lin, and B. S. Ooi, "4-Gbit / s visible light communication link based on 16-QAM OFDM transmission over remote phosphor-film converted white light by using blue laser diode," Optics Express, vol. 23, no. 26, pp. 88–97, 2015.

[39]   "Wireless future drives microwave photonics," Nature Photonics vol. 5, no. 12 p. 724, 2011.

[40]   H. Elgala, "Indoor Optical Wireless Communication : Potential and State-of-the-Art," *IEEE Communications Magazine,* vol. 49 no. 9, pp. 56–62, 2011.

[41]   J. Rufo, "Visible Light Communication Systems for Passenger In-Flight Data Networking," *IEEE International Conference on Consumer Electronics (ICCE)*, IEEE, pp. 445–446, 2011.

[42]   N. Kumar, N. Lourenço, D. Terra, L. N. Alves, R. L. Aguiar, and S. Member, "Visible Light Communications in Intelligent Transportation Systems," *Intelligent Vehicles Symposium (IV)*, *IEEE*, 2012.

[43]   I. Takai, M. Andoh, I. Takai, T. Harada, M. Andoh, and K. Yasutomi, "Optical Vehicle - to - Vehicle Communication System Using LED Transmitter and Camera Receiver Optical Vehicle - to - Vehicle Communication System Using LED Transmitter and Camera Receiver," *IEEE Photonics Journal*, vol. 0655, no. c, pp. 1–14, 2014.

[44]   H. M. Oubei, C. Li, K. Park, T. K. Ng, and B. S. Ooi, "2.3 Gbit / s underwater wireless optical communications using directly modulated 520 nm laser diode," Optics Express, vol. 23, no. 16, pp. 20743–20748, 2015.

[45]   G. Ghione "Semiconductor Devices for High-Speed Optoelectronics,"

Cambridge University Press, 2011.

[46]   G. Cossu, R. Corsini, P. Choudhury, E. Ciaramella, A. M. Khalid, G. Cossu, R. Corsini, P. Choudhury, and E. Ciaramella, "1-Gb / s Transmission Over a Phosphorescent White LED by Using Rate-Adaptive Discrete Multitone Modulation White LED by Using Rate-Adaptive Discrete," *IEEE Photonics Journal*, vol. 4, no. 5, pp. 0–9, 2012.

[47]   C. T. Lin, C. C. Wei, C. W. Chen, Z. Y. Chen, and H. T. Huang, "Performance Comparison of OFDM Signal and CAP Signal Over High Capacity RGB-LED-Based WDM Visible Light Communication Performance Comparison of OFDM Signal and CAP Signal Over High Capacity," *IEEE Photonics Journal*, vol. 5, no. 4, 2013.

[48]   J. J. D. Mckendry, D. Massoubre, S. Zhang, B. R. Rae, R. P. Green, E. Gu, R. K. Henderson, A. E. Kelly, and M. D. Dawson, "Visible-light communications using a CMOS-controlled micro-light-emitting-diode array," *Journal of Lightwave Technology*, vol. 30, no. 1, pp. 61–67, 2012.

[49]   J. J. Wierer, J. Y. Tsao, and D. S. Sizov, "Comparison between blue lasers and light-emitting diodes for future solid-state lighting," *Laser & Photonics Reviews,* vol. 31, pp. 1–31, 2013.

[50]   S. Watson, M. Tan, S. P. Najda, P. Perlin, M. Leszczynski, G. Targowski, S. Grzanka, and A. E. Kelly, "Visible light communications using a directly modulated 422 nm GaN laser diode," Optics Letters, vol. 38, no. 19, pp. 3792–3794, 2013.

[51]   Y. Chi, D. Hsieh, C. Tsai, H. Chen, H. Kuo, and G. Lin, "450-nm GaN laser diode enables high-speed visible light communication with 9-Gbps QAM-OFDM," *Optics Express,* vol. 23, no. 10, pp. 9919–9924, 2015.

[52]   OSRAM Opto Semiconductors "Blue Laser Diode in TO38 ICut Package PL 450B" data sheet, 2013.

Vitae

Name   : Mohamed Adel Shemis

Nationality   : Egyptian

Date of Birth   : 3rd May 1992

Email   : Shemismohamed@gmail.com

Address   : 37 Ali bin Abi Taleb St., Al-Mansoura 33519, Egypt

Academic Background   :

- Master of Science (M.Sc.) in Electrical Engineering, King Fahd University of Petroleum and Minerals, May 2017.

- Bachelor of Science (B.Sc.) in Electrical Engineering, King Fahd University of Petroleum and Minerals, January 2015.

- Bachelor of Science (B.Sc.) in Physics, King Fahd University of Petroleum and Minerals, January 2015.